

Gas-phase and model ice-surface reactions of S(1D) with water and methanol: a computational investigation and implications for cosmochemistry/astrochemistry

Andrea Giustini,[†] Gabriella Di Genova,[‡] Dimitrios Skouteris,[¶] Cecilia Ceccarelli,[§]
Marzio Rosi,[†] and Nadia Balucani^{*,‡}

[†]*Dipartimento di Ingegneria Civile e Ambientale, Università degli Studi di Perugia, 06125
Perugia, Italy*

[‡]*Dipartimento di Chimica, Biologia e Biotecnologie, Università degli Studi di Perugia,
06123 Perugia, Italy*

[¶]*Master-Tec SrL, Via Sicilia 41, 06128 Perugia, Italy*

[§]*Université Grenoble Alpes, CNRS, Institut de Planétologie et d’Astrophysique de Grenoble
(IPAG), 38100 Grenoble, France*

E-mail: nadia.balucani@unipg.it

Abstract

Gas-phase reactions of atomic sulfur in its first electronically excited metastable state, S(1D), with water and methanol have been theoretically investigated to characterize their potential energy surfaces, the reaction mechanisms, and product branching fractions. According to our results, both reactions proceed with the formation of bound intermediates that, for the isolated systems, decompose into products because of the

large energy content with which they are formed. The $\text{SO}(\text{a}^1\Delta) + \text{H}_2$ channel is the only open for the $\text{S}({}^1\text{D}) + \text{H}_2\text{O}$ reaction, while many channels are open for the $\text{S}({}^1\text{D}) + \text{CH}_3\text{OH}$ reaction. For the latter case, statistical estimates of the product branching fractions indicate that the main channels are those leading to $\text{CH}_2\text{OH} + \text{SH}$, $\text{H}_2\text{CO} + \text{H}_2\text{S}$, $\text{H}_2\text{CS} + \text{H}_2\text{O}$, and $\text{CH}_3 + \text{HSO}$. The mechanism of the related $\text{O}({}^1\text{D}) + \text{CH}_3\text{SH}$ reaction has also been unveiled.

Since the reaction intermediates can be stabilized by energy loss to surrounding species on ice or in liquid water, to gain some insight into the possible effects of water molecules we have also analyzed how the two reactions behave when four additional water molecules are added. The conclusion is that the initial intermediates formed by the insertion or addition mechanism – namely HOSH (hydrogen thioperoxide) and H_2OS for $\text{S}({}^1\text{D}) + \text{H}_2\text{O}$ and CH_2OHSH (mercaptomethanol), CH_4OS and CH_3OSH (methyl thioperoxide) for $\text{S}({}^1\text{D}) + \text{CH}_3\text{OH}$, as well as CH_3SOH (methyl sulfenic acid) for $\text{O}({}^1\text{D}) + \text{CH}_3\text{SH}$ – will probably be stabilized by the interaction with the additional water molecules.

Our results can help in understanding sulfur chemistry in space, especially in the case of comets. On one side, the $\text{S}({}^1\text{D}) + \text{H}_2\text{O}$ gas-phase reaction could account for the additional SO source necessary to explain the observed distribution of this species obtained by using the Plateau de Bure interferometer of Institut de Radioastronomie Millimétrique (IRAM) for the Hale Bopp comet. On the other side, some of the S/O-containing molecules identified by ROSINA (Rosetta Orbiter Spectrometer for Ion and Neutral Analysis) during the enhanced dust emission events of the 67/P comet (e.g. species with gross formula HSO , H_2SO , and CH_4OS) could be the results of the chemistry occurring on ice that we have exposed in this work.

1. Introduction

Sulfur, with an atomic fraction of 16 ppm, is the tenth most abundant element in the Solar System. It is one of the six most common elements in living organisms (it belongs to the

CHNOPS group – standing for carbon, hydrogen, nitrogen, oxygen, phosphorus, and sulfur – which together make up more than 96% of the mass of living organisms) and it is present in two (cysteine and methionine) of the twenty amino acids common to all life forms as well as in other important sulfur-bearing biomolecules.

A handful of simple sulfur molecules (*e.g.* H₂S, CS, SO) have been widely detected in the interstellar medium.¹ Other species (*e.g.* SiS, HS, NS, HCS, HSC, HSCN, H₂CS, CH₃SH, C₃S, C₄S, C₅S, H₂CCS, HCCS, CHOSH, CH₃CH₂SH) have been more rarely observed.² Detecting reduced sulfur compounds and organosulfur species in star-forming regions and protoplanetary disks is particularly interesting because of the implications in the chemistry of early Earth. However, when considering the abundance of sulfur compounds in cold prestellar cores, S turns out to be significantly depleted from the gas phase (the “sulfur depletion problem”^{1,3–8}), suggesting its presence in the small dust particles (and their icy mantles) that account for *ca.* 1% by mass of those interstellar regions. However, the main sulfur reservoir species in the dust particles or their icy mantles remains unknown. Currently, OCS is the only S-bearing molecule securely detected in interstellar ice.^{9–12}

The inventory of S-containing species becomes much richer when we consider small objects of the Solar System. Simple species like H₂S, OCS, SO, SO₂, S₂, CS₂, and NS have been identified in the coma of several comets for some years.^{13–23} In the case of the 67/P Churyumov-Gerasimenko comet, the Rosetta orbiter Spectrometer for Ion and Neutral Analysis (ROSINA) was able to identify other species like S₃, S₄, CH₃SH, and C₂H₅SH/CH₃SCH₃.^{24–26} Furthermore, during several enhanced dust emission events (that allowed the release of semivolatile species in the proximity of the instrument) the detection of complex organic molecules including S-bearing species (*e.g.* CH₃OS, CH₄OS, C₂H₄OS)^{27,28} and even ammonium hydrosulfide salt NH₄SH²⁹ was achieved. Very rich is the sulfur chemical inventory of the near-Earth carbonaceous asteroid (162173) Ryugu, the surface material of which was brought to Earth by the Hayabusa2 mission^{30–32} as well as that of meteorites like Murchinson and Allende.³³ Clearly, there is some unknown chemistry converting the

simple S-molecules detected in star-forming regions into the more complex species seen in pristine small objects like comets and asteroids/meteorites. Impacts of these bodies on planets were common during the early history of Earth and may have allowed the delivery of organic molecules from which life emerged.³⁴

Atomic sulfur is characterized by a low-lying metastable electronic state, ¹D (radiative lifetime of 28 s; energy content of 110.5 kJ/mol with respect to the ³P ground state³⁵). In space, it is routinely produced by UV-induced photodissociation of some molecules, such as OCS, CS₂, and S₂,^{36–39} while photodissociation at $\lambda \leq 155$ nm (including the Lyman- α wavelength) of H₂S and SO₂ can also produce directly S(¹D) with a significant quantum yield.^{40–42} Given its short radiative lifetime, S(¹D) is not expected to significantly contribute to the chemical evolution of the most rarefied regions of our Galaxy. However, it might contribute in regions where the number density is higher (e.g. in internal regions of protoplanetary disks or in cometary comae and planetary atmospheres). In addition to that, the reactions of the electronically excited metastable state ¹D of atomic oxygen have been recently invoked to account for the formation of interstellar complex organic molecules in interstellar ice.^{43–46} A similar mechanism could take place starting from the UV-induced photodissociation of OCS (already identified in interstellar ice) or other S-bearing species making S(¹D) reactions on ice a viable route toward the formation of more complex S-molecules. Finally, the reactions of S(¹D) may also be of relevance in atmospheric chemistry. Several reduced sulfur compounds are abundantly released from biogenic sources. Such reduced sulfur compounds are partly converted to OCS, the most abundant atmospheric sulfur species.^{47,48} OCS is a relatively inert species that reaches the upper troposphere/lower stratosphere where it photodissociates in the window between the O₂ and O₃ absorption bands producing CO and S(³P,¹D), with the spin allowed production of S(¹D) being the dominant channel.^{49,50}

In previous work, we reported the study of the reaction mechanism for the systems S(¹D) + C₂H₂, S(¹D) + C₂H₄, and S(¹D) + CH₄.^{51–55} Those reactions were investigated by

means of the crossed molecular beam method with mass spectrometric detection. Electronic structure calculations of the potential energy surfaces (PESs) were also carried out,^{51–55} and statistical estimates of the product branching fractions (BFs) were performed for the multichannel S(¹D) + C₂H₄ reaction.^{51,55} These three reactions were also found to be very fast (the rate coefficients are in the gas kinetic limit also at very low temperatures - as low as 23 K).^{51,52,54} As in the analogous O(¹D)/O(³P) case, from our previous work we learned that S(¹D), besides being much more reactive than S(³P), can undergo insertion reactions (in which the excited atom can position itself into one of the preexisting σ bonds of the reaction partner forming two new sigma bonds) as well as add to the π system of unsaturated hydrocarbons. In this respect, it is also similar to the case of the reactions of other electronically excited states of atomic species, like C(¹D) and N(²D) (see, for instance, Ref.s^{56–61}).

In this manuscript, we extend the same theoretical approach to characterizing the S(¹D) reactions with water and methanol. The choice of these two systems is given by the fact that water is the most abundant molecule in cometary comae as well as in interstellar ice, while CH₃OH also has a significant abundance in both cases.^{9,14,62–64} Contrarily to other electronically excited atomic species (e.g. O(¹D), C(¹D), and N(²D)^{65,66}), S(¹D) has been spectroscopically identified in cometary comae rarely (e.g. in the comet 153P/ Ikeya-Zhang⁶⁷). However, given the fact that so many processes lead to its formation^{36–42} and that its radiative lifetime is not too small³⁵ (the number density in the proximity of the comet nucleus is large enough for it to undergo collisions within its decay), its gas-phase reactions have already been invoked to explain the formation mechanism of some sulfur species^{68,69} in alternative to its physical quenching (considered to be caused mostly by collisions with water molecules).⁷⁰ In addition to that, the results presented here can provide some insight into the possible S(¹D) chemistry on interstellar ice or in atmospheric aerosols containing S(¹D) precursors.

Unfortunately, we cannot investigate the S(¹D) + H₂O reaction experimentally with the

crossed molecular beam method because the heavy product of the only open channel is SO (+ H₂) which is largely present in our atomic sulfur beam produced by radiofrequency discharging a mixture of SO₂ and He^{51–55} and strong interference from elastic scattering is expected. According to our calculations, indeed, the two-product reaction channels are



where the enthalpies of reaction of each channel are those resulting from our calculations at the CCSD(T)/CBS level (in parentheses the accepted values in the literature when available⁷¹). To gain insight into the possible effects of the presence of surrounding water molecules (either in interstellar ice or in atmospheric aerosols), we also derived the reactive potential energy surface in the presence of four additional water molecules forming a small cluster (4WMC). The reaction mechanism significantly changes because of the H-bond interactions and the only possible two-product exit channels (both endothermic) become



where the enthalpies of reaction of each channel are those resulting from calculations at the CCSD(T)/aug-cc-pV(T+d)Z level of theory (see below).

The reaction mechanism for S(¹D) + CH₃OH is much more complex and numerous two-product channels are open. In anticipation of possible experiments with the CMB technique, we have also characterized the reaction mechanism for the related system O(¹D) + CH₃SH. Also in these two cases, we have considered the effect of the presence of four water molecules, but at a lower level of calculations because of the computational cost.

The structure of the manuscript is as follows: In Section 2, we present the methods employed to carry out the electronic structure calculations of the relevant stationary points along the PESs and RRKM estimates of the product BFs for the reaction S(¹D) + CH₃OH. In section 3, we present the main features of the PESs for the two isolated systems and the Rice-Ramsperger-Kassel-Marcus (RRKM) estimates of BFs for the S(¹D) + CH₃OH reaction. In section 4 we present our results for the S(¹D) reaction with water and methanol in the presence of four additional water molecules. In section 5, the discussion and the related astrophysical implications are presented. Conclusions are presented in Section 6.

2. Methods

The relevant potential energy surfaces have been investigated by localizing the stationary points using the ω B97XD functional⁷² in conjunction with the correlation consistent valence polarized set aug-cc-pVTZ,⁷³ augmented with a tight *d* function with exponent 2.457 for the sulfur atoms to correct for the core polarization effects⁷⁴ (we denote this basis set as aug-cc-pV(T+d)Z). At the same level of theory, we have computed the harmonic vibrational frequencies. With the exception of the S(¹D) + CH₃OH reaction with 4WMC, the energy of all the stationary points of the PESs was then computed at the higher level CCSD(T)^{75,76} using the same basis set aug-cc-pV(T+d)Z. Both the ω B97XD and the CCSD(T) energies were corrected to 0 K by adding the zero point energy correction computed using the scaled harmonic vibrational frequencies evaluated at the ω B97XD level. All the structure optimizations and CCSD(T) calculations were performed using the Gaussian 09 program package.⁷⁷

Intrinsic reaction coordinate (IRC) calculations⁷⁸ at the same DFT level of theory were performed to confirm the transition states to be uniquely connected to the local minima and the corresponding reaction products. More accurate calculations were then performed for the isolated H₂OS and CH₄OS systems at the CCSD(T) level corrected with a density-fitted (DF) MP2 extrapolation to the complete basis set (CBS) and with corrections for core electron excitations. Using this algorithm implemented with the Molpro program package,⁷⁹ the energy was computed as follows:

$$E = E(\text{CCSD(T)/aug-cc-pV(T+d)Z}) + [E(\text{CCSD(T,core)/cc-pVTZ}) - \\ - E(\text{CCSD(T)/cc-pV(T+d)Z})] + [E(\text{DF-MP2/CBS/cc-pV(T+d)Z}) - \\ - E(\text{DF-MP2/CBS/aug-cc-pV(T+d)Z})] \quad (3)$$

where the tight *d* function was added to the sulfur basis set, as suggested by Wilson and Dunning.⁸⁰ Martin's two-parameter scheme⁸¹ for extrapolation was also employed. For simplicity, this level of calculations will be denoted CBS in the rest of the paper. Regarding the electronically excited atoms, we added the experimental energy difference between the corresponding ³P ground state and the ¹D excited state to compute the electronic energies of S(¹D) and O(¹D). The adopted values were 110.5 kJ/mol for S(³P)–S(¹D) energy split and 189.5 kJ/mol for O(³P)–O(¹D) split.^{35,82} Since we could not optimize the CH₃S structure using the ωB97XD functional, for this species we have used the B3LYP/aug- cc-pV(T+d)Z method.^{73,74,83,84}

RRKM calculations were performed to estimate the statistical product BFs for the S(¹D)+CH₃OH reaction at various temperatures and zero pressure, using a home-made code developed for this purpose, previously employed for many systems.^{51,56,58,60,61,85} This approach can be applied to bimolecular reactions when one or more bound intermediates are present along the minimum energy path. In the framework of the RRKM theory, a statistical redistribution of the available energy among all the degrees of freedom is taken into account.

The 1-dimensional Master Equation is solved by computing all the relevant microcanonical rate constants and neglecting the effect of angular momentum conservation. The microcanonical rate constants for each unimolecular channel were calculated using the following formula:

$$k(E) = \frac{N(E)}{h\rho(E)} \quad (4)$$

where E is the total energy available to the intermediates, $N(E)$ corresponds to the sum of states of the transition state at energy E , h is the Planck constant, and $\rho(E)$ is the density of states. While $\rho(E)$ was estimated by counting the number of vibrational states per energy range, $N(E)$ was computed by integrating the density of states of the transition state in the specific energy interval $0 - E$. On the other hand, the rotational density of states was estimated using well-known classical expressions (as derived, for example, by an inverse Laplace transform of the corresponding partition functions) and subsequently convoluted with the vibrational ones. We also considered quantum tunneling using the corresponding imaginary frequency of the transition state and simulating the barrier by a symmetric Eckart barrier to calculate the tunneling probability. For the barrierless exit channels, the best treatment of "loose" transition states (monotonic dissociation channels) would be a variational treatment. However, as this approach has proved too demanding given the complexity of the system, we have opted to assume, in these cases, a "product-like" transition state (where product molecule rotations are treated like internal rotations). This approach, in accord with the variational principle, yields an upper bound to the true rate constant. As this transition state corresponds to the maximum energy, the rate constant obtained should not be too far from the true one.

Once branching fractions have been obtained as a function of total energy, these are averaged assuming a prior Boltzmann distribution for the reactants ($S(^1D) + CH_3OH$) at the representative temperatures of interstellar ice and comets (10, 100 K) and at room temperature.

3. Results

3.1 The potential energy surface for the gas-phase S(¹D) + H₂O reaction

The following description will refer to the energy values calculated at the CBS level. The energy values are reported rounded to the nearest kJ/mol considering the accuracy of the calculations. In Figure 1 and in the Supporting Information (SI), the values obtained at the CCSD(T)/aug-cc-pV(T+d)Z level of theory are also shown for comparison because the calculations relative to the same reaction in the presence of four additional water molecules could be carried out only at this level. The comparison between the two sets of values, therefore, is a way to assess the accuracy of the lower-level calculations. The ω B97XD energy values are also shown in the SI for comparison (all energies in hartrees).

As expected, the interaction of S(¹D) with the water molecule starts with two different approaches: *i*) insertion into one of the OH bonds of water or *ii*) addition to one of the lone pairs of the oxygen atom of the water molecule. In both cases, a low-lying bound intermediate is formed (MIN1, located at -98 kJ/mol with respect to the reactants asymptote, for addition and MIN2, located at -258 kJ/mol, for insertion - see Figure 1). In principle, S(¹D) could also abstract one H atom, but the channel leading to OH + SH is endothermic by 32 kJ/mol and cannot contribute under the typical conditions of most environments.

Once formed, MIN1 can easily rearrange to MIN2 by overcoming a barrier of 48 kJ/mol (associated with TS1) or dissociate to the products SO + H₂. In this case, a very high barrier must be overcome (243 kJ/mol), as is typical for a three-center H₂ elimination channel, thus implying that this pathway makes a negligible contribution under common conditions (the associated TS4 is 145 kJ/mol above the reactants energy asymptote). As this is a singlet PES, SO is formed in its lowest singlet state a ¹ Δ rather than in the ground triplet state X ³ Σ^- .

Once formed (either directly by insertion or after the isomerization of MIN1), MIN2 can

dissociate into the products OH + SH (an endothermic channel with $\Delta H_0^o = + 32$ kJ/mol), HSO + H (an endothermic channel with $\Delta H_0^o = + 51$ kJ/mol), HOS + H (an endothermic channel with $\Delta H_0^o = + 65$ kJ/mol) or also isomerize to MIN3 or MIN1. The isomerization to MIN1 does not lead to any exit channel, while the isomerization to MIN3 (located at -188 kJ/mol) finally leads to the only open two-product channel through an accessible exit barrier associated with TS3. Also in this case, the three-center elimination of H₂ is characterized by a very large barrier of 178 kJ/mol which, however, remains below the reactants energy asymptote because of the depth of the potential well associated with MIN3. Therefore, the SO(a ¹ Δ) + H₂ channel is the only open two-product channel.

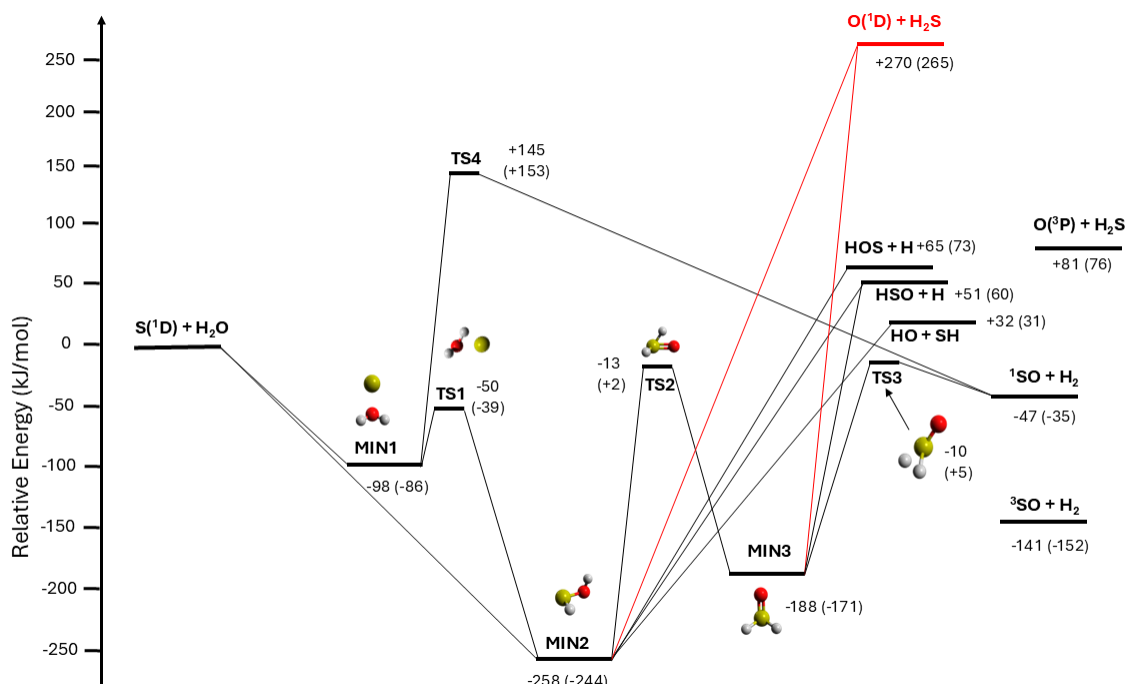


Figure 1: Potential energy surface for the reaction S(¹D) + H₂O calculated at the CBS level of theory on optimized ω B97XD structures. The values obtained at the CCSD(T)/aug-cc-pV(T+d)Z level of theory are also shown in parentheses. The connections with the O(¹D) + H₂S entrance channel are also shown in red.

It is interesting to note that MIN2 and MIN3 are the same intermediates formed in the related reaction O(¹D) + H₂S which has been previously investigated at another level of theory.⁸⁶ If we consider the energy of the stationary points at the G2 level calculated by

Goumri et al.,⁸⁶ starting from the O(¹D) + H₂S asymptote, a value of -369.3 kJ/mol was derived for MIN1, -535.6 kJ/mol for MIN2, and -462.5 kJ/mol for MIN3. For TS1 (TS5 in the paper by Goumri et al.⁸⁶) they obtained a value of -330.6 kJ/mol, for TS2 (TS3 in the paper by Goumri et al.⁸⁶) a value of -294.2 kJ/mol, and for TS3 (TS2 in the paper by Goumri et al.⁸⁶) a value of -294.5 kJ/mol. A very good agreement is noted despite the different theoretical methods employed.

In addition to that, our calculations also nicely reproduce the $\Delta H_{0,r}^\circ$ value of + 30.7 kJ/mol for channel (1b) that can be derived by using the accepted values of $\Delta H_{0,f}^\circ$ for OH and SH.⁷¹ The agreement is also good when considering the difference in energy with respect to the SO product in its ground triplet state (X³ Σ^-) which is - 143.75 kJ/mol (when using the values by Atkinson et al.⁷¹) to be compared with -141 kJ/mol of the present calculations. However, the energy of the excited SO(a¹ Δ) corresponds to 91 kJ/mol to be compared with the accepted value of 77.11 kJ/mol ($T_0=5861\text{ cm}^{-1}$, see Ref.⁸⁷). Therefore, the method employed confirms its problems in dealing with electronic excitation.

The comparison between CBS and CCSD(T)/aug-cc-pV(T+d)Z energy values are in reasonably good agreement with the latter being systematically higher by ca. 10 kJ/mol. To be noted that TS2 and TS3, the transition states that make the SO(a¹ Δ) + H₂ channel open at the CBS level, are slightly above the energy of the reactants asymptote at the CCSD(T)/aug-cc-pV(T+d)Z level of theory while the $\Delta H_{0,r}^\circ$ for the channel (1b) is significantly different with respect to the literature accepted value (-35 kJ/mol vs -66.7 kJ/mol).

3.2 The CH₄OS potential energy surface

The two reactions S(¹D) + CH₃OH and O(¹D) + CH₃SH share a common PES. For this reason, we will describe the reaction mechanism also for the O(¹D) + CH₃SH reaction keeping in mind that, in this case, higher energy TSs and products are accessible because of the extra 226 kJ/mol available to the system. The reaction pathways are sketched in Figures 2 and 3. Because of the complexity of the PES, we have split it into two parts. The

pathways originating by each intermediate are reported only once but they are present for both schemes. In both figures, the energy of the S(¹D) + CH₃OH reactants is assumed as the zero of energy.

3.2.1 The gas-phase S(¹D) + CH₃OH reaction

As expected, the S(¹D) + CH₃OH reaction can start with different approaches: *a*) S(¹D) can insert into one of the C–H bonds of the methyl group of methanol forming the W1 intermediate (mercaptomethanol, W1); *b*) S(¹D) can add to one of the lone pairs of the oxygen atom of methanol forming the W2 intermediate; *c*) S(¹D) can insert into the O–H bond of methanol forming W5 (methyl thioperoxide). W1, W2, W5, and W4 (methyl sulfenic acid, that can be formed by the isomerization of W2 or by the O(¹D) reaction with methanethiol) are associated with deep wells and are singlet closed-shell species. Their structures are shown in Figure 4 together with those of the relevant transition states and the structures of the unusual molecular products that can be formed in the reaction.

We will comment now on the possible fate of these intermediates.

Once formed, W1 evolves through the pathways illustrated in Figure 2 (red lines) and reported in Table 1. In particular, by overcoming a barrier associated with either TS1, TS4, TS2, TS3, or TS5, W1 can *i*) eliminate a molecule of water forming either thioformaldehyde (in a very exothermic channel) or its isomer thiohydroxycarbene; *ii*) eliminate a molecule of hydrogen sulfide forming formaldehyde (in a very exothermic channel) or its isomer hydroxycarbene; *iii*) eliminate an H₂ molecule forming thioformic acid; this channel is very exothermic, but it is inhibited by the presence of a very high barrier associated with a 3-center elimination mechanism.

Alternatively, W1 can dissociate into products in barrierless channels where one of its bonds smoothly weakens before breaking apart and forming *iv*) hydroxymethyl + SH if the newly formed C–S bond breaks apart; *v*) CH₂OSH (P1) + H if the preexisting O–H bond breaks apart (for the detailed structure of CH₂OSH see P1 in Figure 4); *vi*) CH₂SH

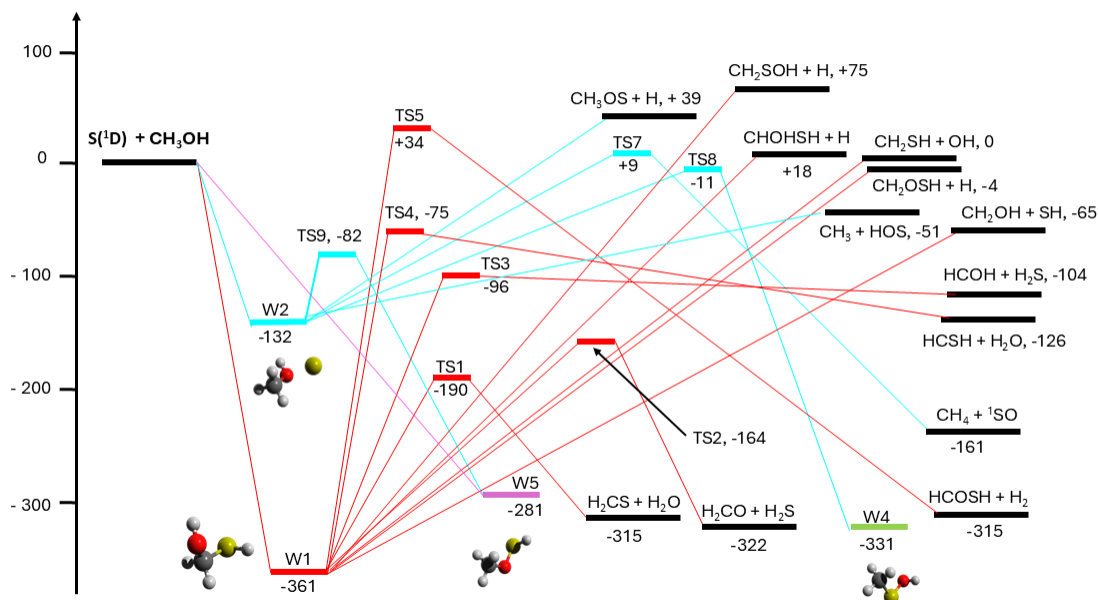


Figure 2: Potential energy surface for the reaction $S(^1D) + CH_3OH$ calculated at the CBS level of theory on optimized ω B97XD structures. The evolution of W4 and W5 is shown in Figure 3.

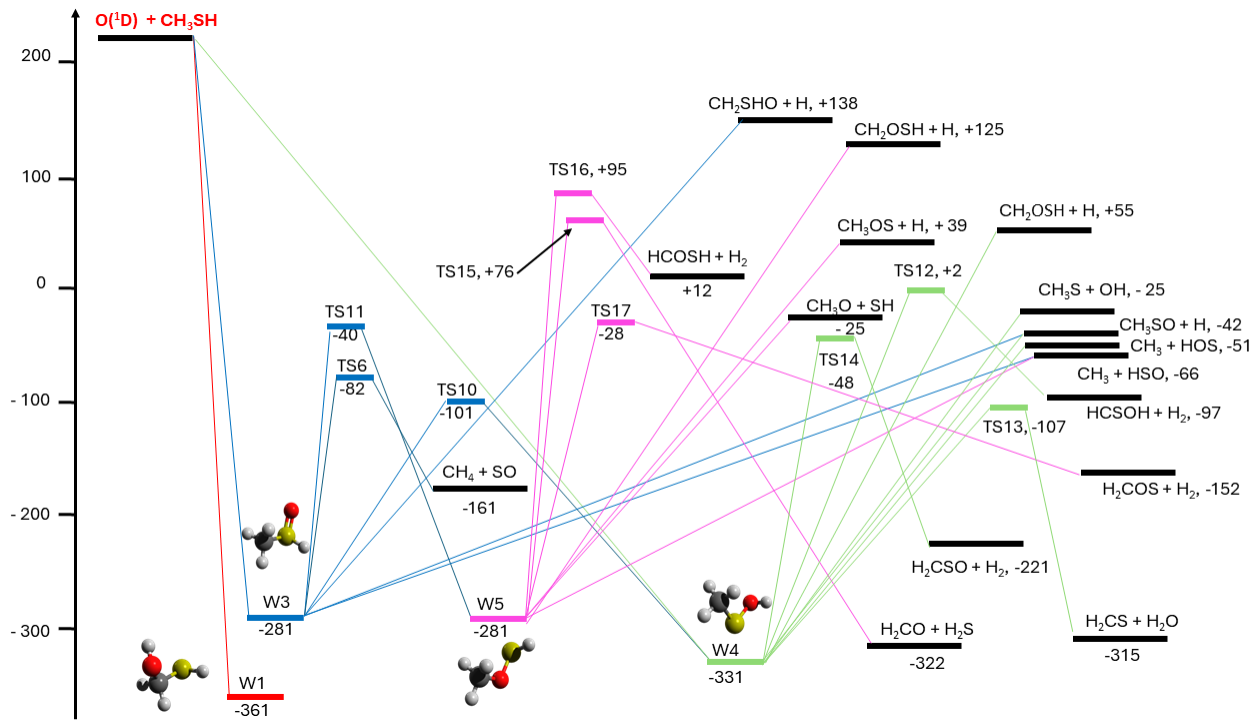


Figure 3: Potential energy surface for the reaction $O(^1D) + CH_3SH$ calculated at the CBS level of theory on optimized ω B97XD structures. The evolution of W1 is shown in Figure 2.

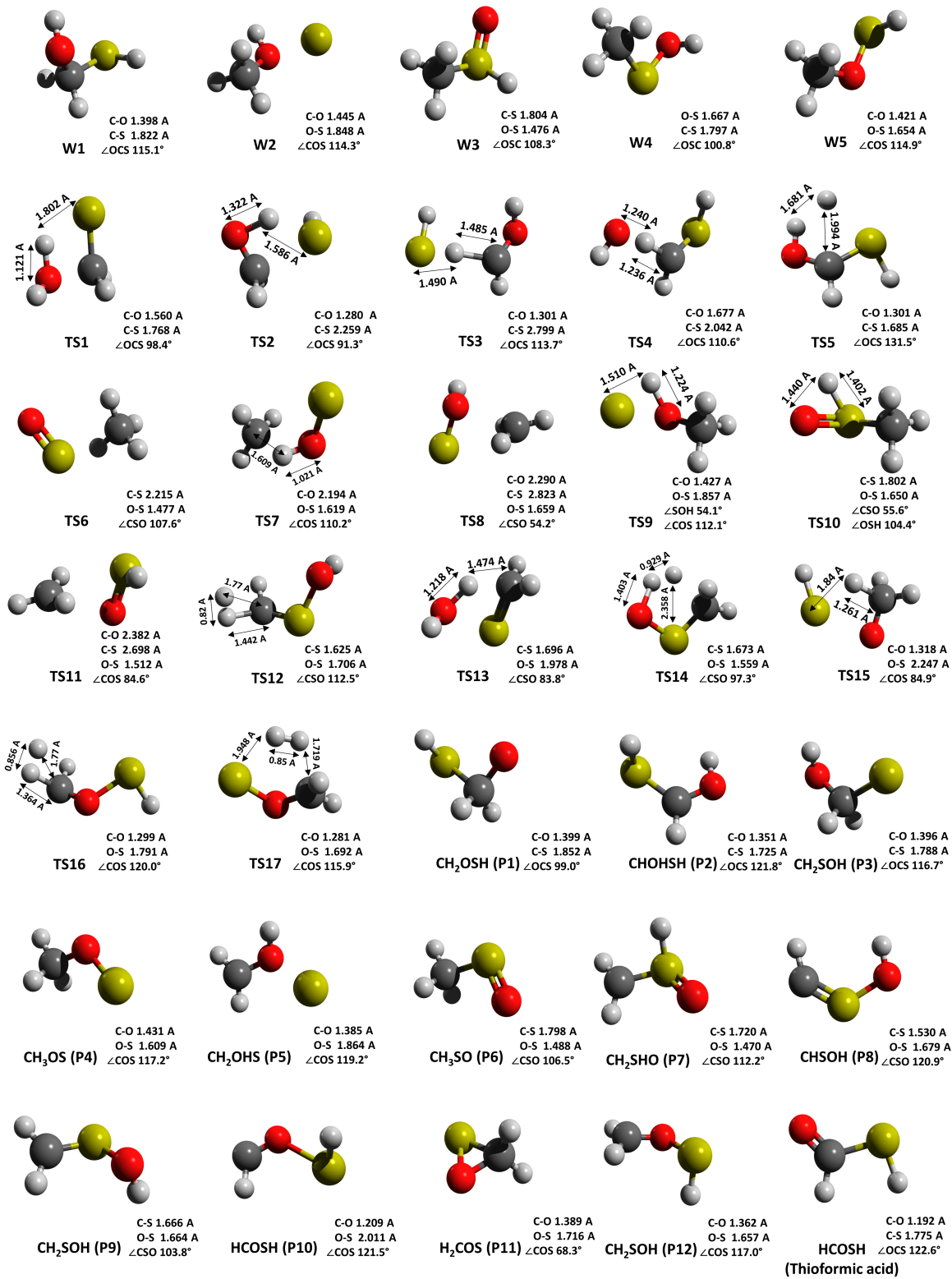


Figure 4: ω B97XD-optimized structures of selected intermediates, TSs, and products for the CH_4OS system. Bond lengths are expressed in Angstrom.

(sulfanylmethyl) + OH if the preexisting C–O bond breaks apart; *vii*) CHOHS (P2) + H if one of the preexisting C–H bonds breaks apart (for the detailed structure of CHOHS see P2 in Figure 4); *viii*) CH₂SOH (P3) + H if the newly formed S–H bond breaks apart (see Figure 4 for the structure of P3). The last two channels are endothermic for the S(¹D) + CH₃OH reaction but are exothermic for the O(¹D) + CH₃SH (W1 can also be formed by the insertion of O(¹D) into one of the C–H bonds of methanethiol).

The evolution of W2 is much simpler (see Figure 2, cyano lines). It either isomerizes to W5 or W4 (by overcoming a barrier of 50 kJ/mol or 121 kJ/mol, respectively) or it dissociates into CH₃ + HOS by the breaking of the preexisting C–O bond or into CH₃OS (P4 in Figure 4) + H by the breaking of the preexisting O–H bond (however this last channel is significantly endothermic). Finally, overcoming a significant barrier of 141 kJ/mol (TS7), W2 can evolve toward CH₄ and SO(a¹Δ) in a very exothermic channel. The associated TS7 suggests that the methyl moiety abstracts an H atom from HOS while they separate. However, the barrier is above the reactants energy and this channel is not expected to contribute appreciably. A last possibility is associated with the formation of CH₂OHS (P5 in Figure 4) + H if one of the preexisting C–H bonds breaks apart. This channel is endothermic by 299 kJ/mol and is not shown in Figure 2.

The evolution of W4 and W5 is shown in Figure 3 (green lines and magenta lines, respectively). W5 (which can be formed directly by the insertion of S(¹D) into the O–H bond of methanol or by the isomerization of W2) can: *i*) eliminate a molecule of hydrogen sulfide forming formaldehyde; *ii)-iii*) eliminate an H₂ molecule forming either HCOSH (P10 in Figure 4) or H₂COS (P11 in Figure 4), that is, two isomers of thioformic acid; the formation of P10 is possible after overcoming the very high barrier associated with a 3-center elimination mechanism (see TS16), while the 5-center elimination of H₂ requires the overcoming of a much smaller barrier (TS17).

Alternatively, W5 can dissociate into products in barrierless channels where one of its bonds smoothly weakens before breaking apart and forming *iv*) methoxy + SH if the newly

Table 1: List of the reaction pathways in the CH₄OS PES with the corresponding reaction enthalpies at 0 K relative to S(¹D) + CH₃OH (in kJ/mol). The reaction enthalpies calculated with previously published $\Delta H_{0,f}^\circ$ are also shown.^{88–90} When not available at 0 K, we indicated the reaction enthalpy at 298 K.

Intermediate	Reaction Pathway	$\Delta H_{0,r}^\circ$ (CBS)	$\Delta H_{0,r}^\circ$ (literature)
W1	TS1 → H ₂ CS (Thioformaldehyde) + H ₂ O	-315	-317.8
W1	TS2 → H ₂ CO (Formaldehyde) + H ₂ S	-322	-320.1
W1	TS3 → HCOH _{cis} (Hydroxycarbene) + H ₂ S	-104	-102
W1	TS4 → HCSH _{trans} (Thiohydroxycarbene) + H ₂ O	-126	-
W1	TS5 → HCOSH (Thioformic acid) + H ₂	-315	-
W1	→ CH ₂ OH (Hydroxymethyl) + SH (Sulfanyl)	-65	-65
W1	→ CH ₂ OSH (P1) + H	-4	-
W1	→ CH ₂ SH (Sulfanylmethyl) + OH	+0	+5.2
W1	→ CHOHS (P2) + H	+18	-
W1	→ CH ₂ SOH (P3) + H	+75	-
W2	TS7 → CH ₄ + SO(a ¹ Δ)	-161	-186.8
W2	→ CH ₃ OS (P4) + H	+39	-
W2	→ CH ₃ + HOS	-51	-49.9
W2	→ CH ₂ OHS (P5) + H	+299	-
W3	TS6 → CH ₄ + SO(a ¹ Δ)	-161	-186.8
W3	→ CH ₃ + HSO	-66	-67.1
W3	→ CH ₃ SO (Methylsulfinyl) (P6) + H	-42	-41 ($\Delta H_{298,r}^\circ$)
W3	→ CH ₂ SHO (P7) + H	+138	-
W4	TS13 → H ₂ CS (Thioformaldehyde) + H ₂ O	-315	-317.8
W4	TS14 → H ₂ CSO (Sulfinylmethane) + H ₂	-221	-225.7
W4	TS12 → HCSOH (P8) + H ₂	-97	-
W4	→ CH ₃ SO (Methylsulfinyl) (P6) + H	-42	-41 ($\Delta H_{298,r}^\circ$)
W4	→ CH ₃ + HOS	-51	-49.9
W4	→ CH ₃ S (Methylsulfanyl) + OH	-29 ^a	-26.9 ($\Delta H_{298,r}^\circ$)
W4	→ CH ₂ SOH (P9) + H	+55	-
W5	TS15 → H ₂ CO (Formaldehyde) + H ₂ S	-322	-320.1
W5	TS16 → HCOSH (P10) + H ₂	+12	-
W5	TS17 → H ₂ COS (P11) + H ₂	-152	-
W5	→ CH ₃ + HSO	-66	-67.1
W5	→ CH ₃ O (Methoxyl) + SH (Sulfanyl)	-25	-25.6
W5	→ CH ₃ OS (P4) + H	+39	-
W5	→ CH ₂ OSH (P12) + H	+125	-

^a ZPE correction of CH₃S at the B3LYP/aug-cc-pV(T+d)Z level of theory.

formed O–S bond breaks apart; *v*) CH₃OS + H if the newly formed S–H bond breaks apart (this channel is endothermic for the S(¹D)+H₂O reaction); *vi*) CH₃ + HSO if the preexisting C–O is broken; *vii*) CH₂OSH (P12, see Figure 4) + H if the preexisting C–H bond is broken.

W4 can, instead, *i*) eliminate a molecule of water forming thioformaldehyde; *ii*) eliminate an H₂ molecule forming either H₂CSO(sulfinylmethane) or HCSOH (P8 in Figure 4), two isomers of thioformic acid. Alternatively, W4 can dissociate into products in barrierless channels where one of its bonds smoothly breaks apart, thus forming *iv*) CH₃S (Methylsulfanyl) + OH, *v*) CH₃ + HOS, *vi*) CH₃SO (P6, Figure 4) + H, and *vii*) CH₂SOH (P9, Figure 4) + H.

3.2.2 The gas-phase O(¹D) + CH₃SH reaction

O(¹D) can *a*) insert into one of the C–H bonds of the methyl group of methanethiol forming the W1 intermediate; *b*) add to one of the lone pairs of the sulfur atom of methanethiol forming the W3 intermediate; *c*) insert into the S–H bond of methanethiol forming W4. The evolution of W1 and W4 has already been commented on above, so only the pathways originating from W3 are described here (see Figure 3).

The W3 intermediate formed by the addition of O(¹D) to the sulfur atom of methanethiol is much more stable than W2 (the equivalent addition intermediate for the reaction S(¹D) + CH₃OH), being associated with a deep well of 281 kJ/mol rather than 132 kJ/mol as was the case of W2 (maintaining S(¹D) + CH₃OH as the zero of energy). As in the case of W2, isomerization to W4 and W5 are possible pathways via TS10 (located at - 327 kJ/mol with respect to the O(¹D)+CH₃SH initial energy) and TS6 (located at - 308 kJ/mol). W4 and W5 evolve in the same way described for the S(¹D)+CH₃OH reaction but the extra energy of 226 kJ/mol can alter the relative product branching fractions (not derived here since they are beyond the scope of this paper). W3 can also decompose into CH₄ and SO(a¹Δ) via TS11 (-186 kJ/mol, see the structure in Figure 4). Alternatively, it dissociates into CH₃SO (Methylsulfanyl) + H by the breaking of the preexisting S–H bond in an exothermic O/H

exchange channel or into $\text{CH}_3 + \text{HOS}$ by the breaking of the preexisting C–S bond. Finally, by the breaking of one of the preexisting C–H bonds, CH_2SHO (P7 in Figure 4) + H can be formed.

3.3 RRKM branching fractions for the gas-phase $\text{S}({}^1\text{D}) + \text{CH}_3\text{OH}$ reaction

In the case of the gas-phase $\text{S}({}^1\text{D}) + \text{H}_2\text{O}$ reaction, there is only one open channel and there is no need to establish the product BFs. On the contrary, the reaction with CH_3OH is quite complex as more than one intermediate can be formed by the initial approach of $\text{S}({}^1\text{D})$ with methanol and all of them have more than one open dissociation channel. For this reason, we decided to analyze the reactive system with a statistical approach. Since it is impossible to quantify how the reactive flux is distributed among W1, W2, and W5 without some strong assumption, we preferred to follow the evolution of each initial intermediate separately. The results are summarized in Table 2, while the unimolecular decomposition (or isomerization when relevant) rate coefficients for W1 and W5 are shown in Figures 5 and 6, respectively.

At all the energies considered, the dominant decomposing channels of W1 are those leading to $\text{CH}_2\text{OH} + \text{SH}$, $\text{H}_2\text{CO} + \text{H}_2\text{S}$, and $\text{H}_2\text{CS} + \text{H}_2\text{O}$. The rate constant of the second H_2S elimination channel accompanied by the formation of hydroxycarbene is not negligible. The rate constant for the $\text{CH}_2\text{SH} + \text{OH}$ channel exhibits a strong increase with the total energy but becomes significant only above 50 kJ/mol. All the other channels make a negligible contribution, including the back-dissociation to the reactants. The resulting BFs at 10, 100, and 300 K show a mild dependence on the temperature, with the BF of $\text{CH}_2\text{OH} + \text{SH}$ increasing with the increase of the available energy. These results might seem surprising, as the barrierless channel leading to $\text{CH}_2\text{OH} + \text{SH}$ (which is, actually, slightly dominant at all the energies/temperatures investigated) is associated with a value of reaction enthalpy which is much above the energy of the barriers associated with the H_2O and H_2S elimination channels (TS1 and TS2). However, the (quasi)formation of bimolecular products for monotonic

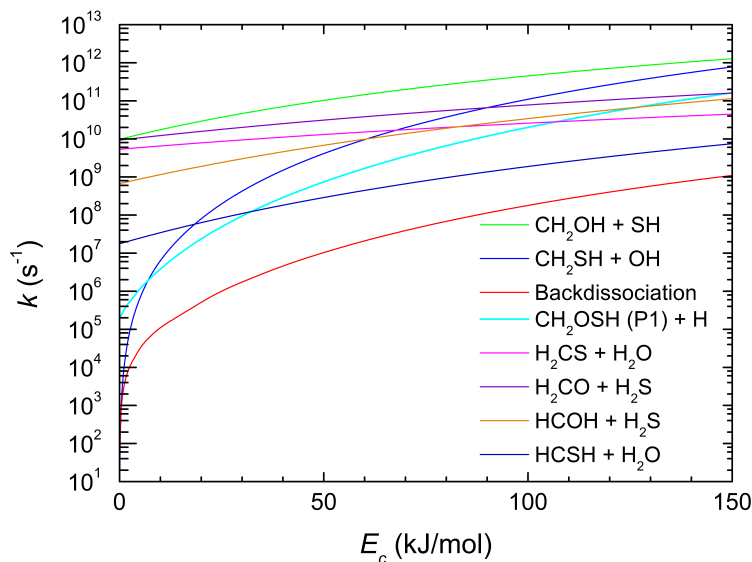


Figure 5: W1 unimolecular decomposition rate constants for each exothermic channel as a function of the collision energy, E_c , of the approaching reactants ($S(^1D)$ + CH_3OH).

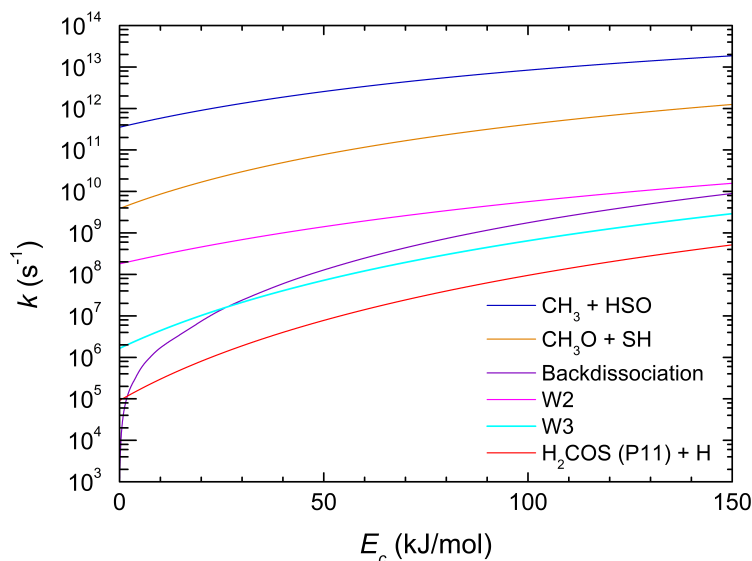


Figure 6: W5 unimolecular decomposition and isomerization rate constants as a function of the collision energy, E_c , of the approaching reactants ($S(^1D)$ + CH_3OH).

dissociation channels is entropically favored with respect to the case of well-defined TS with only vibrational modes because, in the first case, some vibrations turn into quasi-internal rotations and the density of states increases favoring the corresponding products. We remind that a variational treatment of this channel will provide a more reliable rate constant and that the present values should be seen only as upper bounds. However, we do not expect the importance of this channel to be significantly reduced. At very low energies/temperatures, as suggested by energetic considerations, the H₂CO + H₂S and H₂CS + H₂O channels become as important as the CH₂OH + SH channel.

All the reactive flux associated with the formation of the W2 addition intermediate is channeled into W5 since the other channels (including the isomerization to W4) cannot compete. W5, in turn, dissociates almost exclusively into CH₃ + HSO with a very small yield for the CH₃O + SH channel. As visible in Figure 6, the rate constant for the CH₃ + HSO channel is dominant for all the energies considered. As a consequence, the BFs are temperature-independent. All the other channels have a negligible BF, which is not surprising once considering the associated high energy barriers that make them non-competitive.

In conclusion, despite the complexity of the overall PES, just a few channels are important, and these are CH₂OH + SH, H₂CO + H₂S, H₂CS + H₂O, and CH₃ + HSO.

4. The effects of a small cluster of water molecules

4.1 The S(¹D) + H₂O reaction in the presence of four additional water molecules

The PES relative to S(¹D) interacting with a cluster of five water molecules is shown in Figure 7. The reported values of energy have been obtained at the CCSD(T)/aug-cc-pV(T+d)Z level of theory on optimized ω B97XD structures. In preliminary work, we have characterized

Table 2: RRKM branching fractions for the decomposition of the initial W1, W2, and W5 initial intermediates of the S(¹D) + CH₃OH reaction at the indicated values of temperature (at all energies and temperature W2 was seen to completely isomerize to W5).

W1			
Channel	BF (10 K)	BF (100 K)	BF (300 K)
CH ₂ OH + SH	0.39	0.41	0.46
H ₂ CO + H ₂ S	0.37	0.36	0.33
H ₂ CS + H ₂ O	0.21	0.20	0.18
HCOH + H ₂ S	0.03	0.03	0.03

W2, W5	
Channel	BF (10 - 300 K)
CH ₃ + HSO	0.99
CH ₃ O + SH	0.01

the same system at the B3LYP/aug-cc-pV(T+d)Z level of theory. A similar picture emerged from that work, but the energy levels are somewhat different because of the lower level of theory employed.⁹¹

We have chosen this approach to gain insight into the effect of the surrounding water molecules but it is a very simplified version of the real conditions that will be typical in the context of interstellar ice or atmospheric water droplets. Considering the S(¹D) addition mechanism on the lone pair of the O atom, it is immediately evident that the presence of four additional molecules significantly increases the stability of the addition intermediate (MIN1-4WMC) with respect to its reactants (here the zero energy corresponds to the separated S(¹D) and the cluster of five water molecules) when compared to the case of the isolated system (the energy levels, in this case relative to the S(¹D) + a single water molecule, are also shown in Figure 7 in blue for a direct comparison). Such a stabilizing effect is minimal in the case of MIN2-4WMC (-250 with respect to -244 kJ/mol) while it is null in the case of MIN3-4WMC (-171 wrt -170 kJ/mol).¹ That simply means that the presence of four additional

¹For this species we have used the structure optimized at the B3LYP/aug-cc-pV(T+d)Z level of theory

water molecules might stabilize both the configuration of the reactants and that of the intermediates at the same level. The large stabilization effect for the addition intermediate MIN1-4WMC can be understood if one considers the H-bonds that the added sulfur can form with another water molecule. A significant reduction of the relative energy of TS1 can, instead, be explained by the fact that at least another water molecule participates in the isomerization process. Similar effects are seen also for TS2/TS2-4WMC and MIN3/MIN3-4WMC.

However, the most significant effects are seen in other aspects of this reactive system. First of all, we could not locate the transition state connecting MIN3-4WMC to the only exothermic channel of the isolated $S(^1D) + H_2O$ reaction, that is the channel leading to $SO(a^1\Delta) + H_2$. This can be easily rationalized by considering that the H_2 elimination occurs via a 3-center mechanism that requires a huge distortion of the structure of MIN3. The presence of H-bonds with the additional water molecules severely contrasts the necessary distortion of MIN3-4WMC and the $SO(a^1\Delta) + H_2$ channel is not open in this case. Furthermore, MIN2-4WMC does not seem to undergo fission of the O–S bond toward OH + SH because the H-bond structure of MIN2-4WMC would need to open up. Another interesting effect is the inversion of stability for the two isomers HSO/HOS: in the presence of 4WMC, the HOS moiety is able to establish much stronger H-bonds with its O-H termination with respect to HSO where the H atom is bound to sulfur.

In conclusion, when considering the $S(^1D) + H_2O$ reaction in the presence of four additional water molecules, the system does not have any two-product exothermic exit channel. Therefore, our study indicates that either MIN1 or MIN2 will be stabilized in the ice or liquid water matrices. Considering the relative stability, HOSH (hydrogen thioperoxide) is expected to be the main product of the reaction when additional water molecules are considered.

of Ref.⁹¹ because we could not optimize it at the ω B97XD level

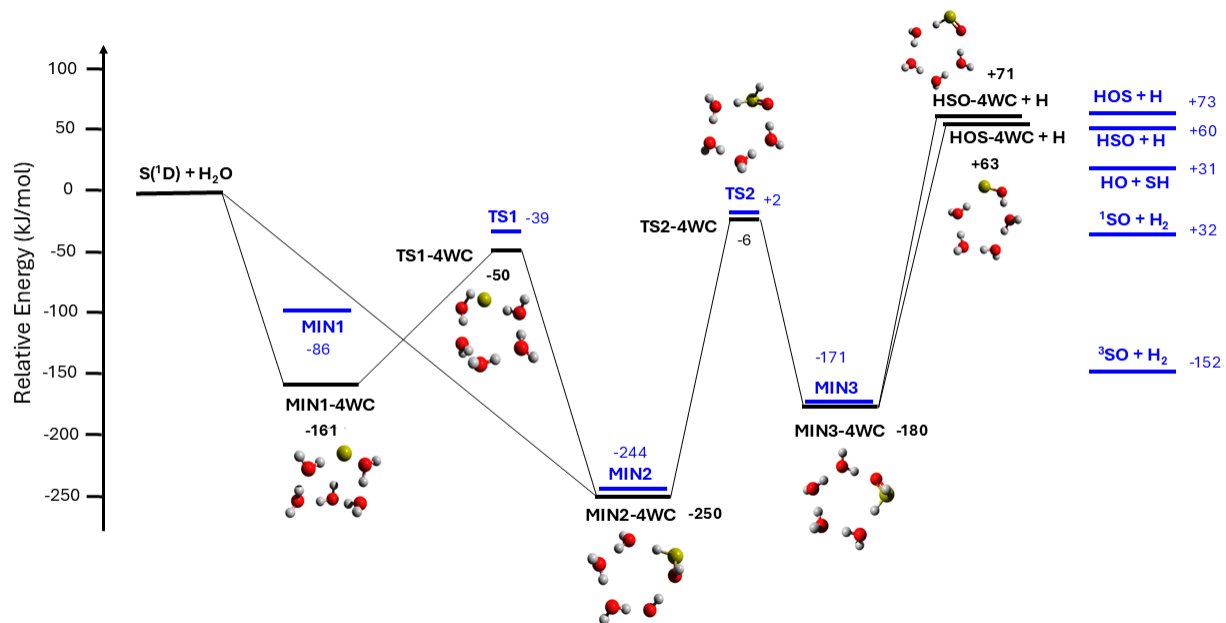


Figure 7: Potential energy surface for the reaction involving $S(^1D)$ and five water molecules calculated at the CCSD(T)/aug-cc-pV(T+d)Z level of theory on optimized ω B97XD structures.

4.2 The $S(^1D)$ + CH_3OH reaction in the presence of four water molecules

Given the complexity of the $S(^1D)$ + CH_3OH system, we could not perform electronic structure calculations at the CCSD(T)/aug-cc-pV(T+d)Z level for the species of interest in the presence of 4WMC. Therefore, we have derived the optimized structures and energies only at the ω B97XD level. However, to check the accuracy of the calculations, we have computed the energy of W1-4WMC also at CCSD(T)/aug-cc-pV(T+d)Z and CBS levels. For the relative energy with respect to the reactants, we obtained the values -369, -355, -371 kJ/mol at ω B97XD, CCSD(T) and CBS levels, respectively. This suggests that the ω B97XD level of calculation is a good compromise between accuracy and computational cost. Also for other systems, we have observed that ω B97XD can be preferred to CCSD(T) for some error compensation.⁹²

In addition, we failed to locate any of the transition states seen for the isolated system. The structures of the W1, W2, W3, W4, and W5 intermediates when interacting with four additional water molecules are shown in Figure 8. All the other structures are shown in Figure S2 of the SI; the energy values are shown in Table S4 of the SI.

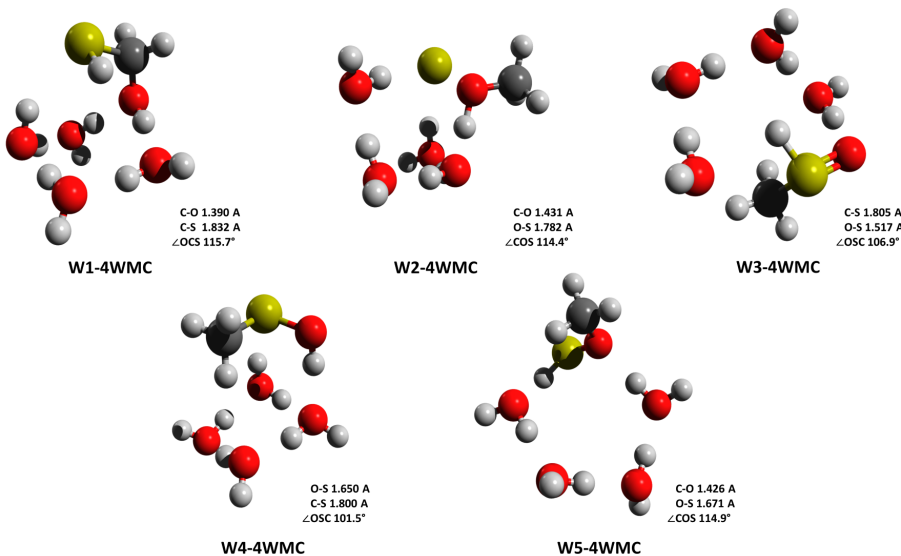


Figure 8: ω B97XD-optimized structures of intermediates W1, W2, W3, W4, and W5 for the $S(^1D) + CH_3OH$ reaction in the presence of additional four water molecules. Bond lengths are expressed in Angstrom. More details are available in the SI.

Considering what we have seen in the case of the $S(^1D) + H_2O$ system, we can suggest that all the exit pathways characterized by a significant energy barrier will be strongly inhibited if an important distortion of the structure of the intermediates is necessary because of the presence of stabilizing H-bonds with the additional water molecules. However, some TSs could also be lowered if the water molecules help in the rearrangement (in particular, if the water molecules participate in a proton transfer process).

Among the channels that are not characterized by an exit barrier, the channel that was dominant for W1 in the gas phase ($CH_2OH + SH$) remains exothermic (see Table S3 in the SI; we have considered two possibilities: either CH_2OH remains bound to the 4WMC and SH is released in the gas phase or SH remains bound to the 4WMC and CH_2OH is lost: in both cases, the ΔH_0° remains negative being - 53 kJ/mol in the first case and -47 kJ/mol in

the second case) as well as the dominant CH₃+HSO channel for W5 (in this case only HSO-4WMC + CH₃ was considered since the binding energy of CH₃ to water ice is quite small⁹³). In general, the final outcome will depend on the capability of the initial intermediates (W1, W2, and W5 for S(¹D) + CH₃OH; W1, W3, and W4 for O(¹D) + CH₃SH) to lose part of the excess energy with which they are formed by the addition/insertion process via the weak interactions with the surrounding water molecules. These processes might be very fast as recently demonstrated by a theoretical approach based on molecular dynamics.^{94,95} Therefore, even if we cannot exclude that the CH₂OH + SH (from W1) and CH₃+HSO (from W5) two-product channels could have a certain yield, it is reasonable to assume that W1, W2, and W5 (as well as W3 and W4 for the O(¹D) + CH₃SH reaction) will be stabilized as such in the ice or liquid water matrix. A further observation could be that the CH₂OH + SH channel from W1 might experience an unfavorable influence from the surrounding water molecules as observed for the OH + SH channel in the reaction S(¹D) + H₂O, while the elimination of the CH₃ moiety from W5-4WMC with the production of HSO-4WMC should not be hindered because of the small binding energy of CH₃.⁹³

5. Discussion

In previous work, we have already seen that S(¹D) has the capability of inserting into σ bonds (see, for instance, the reaction S(¹D) + CH₄⁵⁴) and adding to the π system of unsaturated hydrocarbons (see the cases of S(¹D) + C₂H₂ and C₂H₄^{51,52}). In both systems investigated here, we see that S(¹D) can also efficiently add to one of the lone pairs of oxygen. This was already observed with another insertive species, namely N(²D), as in its reaction with H₂O and CH₃OH also the addition to the lone pair of atomic oxygen was observed^{59,96,97}. It is interesting to compare the N(²D) reactions with those of S(¹D). In the case of N(²D) + H₂O, the characteristics of the PES are qualitatively very similar, but the reactive channels leading to HNO + H, HON + H, and OH + NH are all exothermic. This diminishes

the importance of the H₂ elimination channel which, indeed, was found not to occur. For that system, a quasiclassical trajectory (QCT) investigation was pursued and the dynamical description of the system was given. According to that study, the only fate of the H₂ON addition intermediate is isomerization to the insertion intermediate HONH. The QCT results also showed a marked deviation from the expected statistical behavior, posing a caveat to the uncritical application of a statistical approach for small systems despite the presence of deep energy wells along the minimum energy path.^{59,96} In the case of the N(²D) + CH₃OH reaction, a PES was derived where only the insertion into one of the C–H bonds of methanol or the addition to the lone pair of atomic oxygen were considered.⁹⁷ Similar exit channels are also present (e.g. CH₃ + HNO, CH₃O + NH, CH₂OH + NH). However, the statistical estimate of BFs was not pursued and, therefore, we cannot compare the product branching fractions. Furthermore, for that system, a small entrance barrier for the insertion mechanism was identified.⁹⁷

To the best of our knowledge, no rate coefficients are available for the S(¹D) + H₂O and S(¹D) + CH₃OH reactions. According to our calculations, they are expected to be fast, in the gas kinetics limit as observed for many other S(¹D) reactions^{52–54,98,99} because all the barriers along the pathways of the main channels discussed above are below the energy of the reactants. In the case of the reaction with H₂O, two TSs that must be overcome to reach the only two-product open channel are very close to the energy of the reactants being located at -13 (TS2) and - 10 (TS3) kJ/mol at the highest level of calculations employed. Given the expected accuracy of the method (± 5 kJ/mol), both seem to lie below the zero energy. In addition, our calculations derive an energy too high for the product asymptote, so that, if there is an indication that comes from the comparison with known $\Delta H_{0,f}^o$'s,^{71,87} it is that the energy of TS3 approximates the real one from above. Nevertheless, the presence of high energy barriers could increase the rate of back-dissociation to the reactants thus partly reducing the reactive flux toward product formation.

A final comment needs to be made about the occurrence of intersystem crossing to the

triplet PES. This is certainly a possibility because the presence of sulfur increases spin-orbit coupling. While recent experiments on several reactions involving S-species proved the occurrence of ISC,^{100–102} detailed observables from crossed molecular beam experiments on the related O(³P,¹D) + H₂S reactions could not identify any signature of the occurrence of intersystem crossing^{103,104} (as seen, instead, for other reactions involving O(³P,¹D) and investigated with the same experimental approach).^{105–107} However, the significantly lower amount of energy available to the S(¹D) + H₂O system with respect to O(¹D) + H₂S might still increase the probability of ISC. In the models of cometary chemistry, physical quenching to S(³P) via ISC has always been considered the only outcome for the S(¹D) + H₂O collisions.^{68–70} However, after contrasting indications,^{98,99} the S(¹D) physical quenching does not seem to be competitive with two-product reactions as recently demonstrated by CRESU experiments on the S(¹D) + Ar collisions.¹⁰⁸ A conservative estimate of the rate coefficient to be employed in the models of cometary chemistry could be in the $5 \times 10^{-11} - 10^{-10}$ cm³ s⁻¹ range in the 20 – 300 K temperature range.

In the case of the reaction with methanol, instead, we expect a fast evolution toward the products for any initial approach and the rate coefficient of S(¹D) + CH₄ (ca. 2×10^{-10} cm³ s⁻¹ in the range of temperature between 23 and 298 K) can be taken as a sort of lower limit because methanol is a polar molecule.⁵⁴

Motivated by the deep wells associated with the reaction intermediates, we have also scrutinized whether radiative association could occur for both the gas-phase S(¹D) + H₂O and S(¹D) + CH₃OH reactions. We have employed the method developed by Herbst^{109,110} Given the presence of exothermic two-product channels, radiative association did not result to be competitive and cannot give an important contribution.

Concerning the implications in astrochemistry/cosmochemistry, we can conclude that these reactions in the gas phase do not lead to an increased degree of complexity of S-bearing species. The reaction with water only leads to SO while the reaction with methanol mostly converts S(¹D) into SH, H₂S and HSO with only a small fraction of the global yield

associated with H₂CS. Considering that most of S(¹D) is produced by the photodissociation of CS₂, OCS, and H₂S we can conclude that it will be either recycled back to H₂S or actually contribute to the loss of species holding a C–S bond. Interestingly, a recent analysis of SO interferometric observations in Comet C/1995 O1 (Hale-Bopp) concluded that there must be an additional source of SO since the photodissociation of SO₂ alone cannot account for the observed distribution.¹¹¹ This additional source has not been identified yet. Considering the overwhelming abundance of water and all the sources of S(¹D) (most of which are not properly included in the models yet), the S(¹D) + H₂O reaction could be the missing source of SO. The gas-phase S(¹D) + CH₃OH reaction, instead, could be the source of the detected HSO²⁸ (another important source could be the O(¹D) + H₂S reaction)^{103,104} while for the other main products (SH, H₂S, H₂O, H₂CO, CH₂OH, and H₂CS) there are other efficient sources.

The situation is more interesting if we consider the possible outcome in the presence of ice. In those cases, species like hydrogen thioperoxide, mercaptomethanol, methyl thioperoxide (and methyl sulfenic acid in the case of the related O(¹D) + CH₃SH reaction) are formed. These are singlet stable closed-shell species engaged in strong H-bonds with the water ice matrix, which might survive for a long time and accumulate in the ice. In the presence of a flux of H atoms (as in the case of interstellar ice) they do not undergo hydrogenation while possible H-abstraction processes will cause the formation of radicals that will be easily hydrogenated back (see, for instance, Ref.¹¹²). These results could be of great importance in interpreting what Rosetta recorded during the famous event of dust emission from comet 67P on September 5, 2016. During this event, Rosetta was hit by a chunk of ice and dust that increased locally the gas density. ROSINA recorded, in addition to the usual sulfur-bearing species, a plethora of different molecules never seen before. The interpretation was that the sublimation of semivolatile matter inside the equilibrium chamber of ROSINA (T= 273 K) caused the increase of the signal of all the sulfur species already detected (only the signal associated with OCS and CS₂ did not increase during the event) and the appearance of new

species in the mass spectrum. Among them, molecules containing both sulfur and oxygen (that can be described by the general formula $C_nH_mO_lS$, where n can vary between 0 and 3, m between 0 and 6, and l between 1 and 2) were identified. In this group, there are SO, HSO, H_2SO , and CH_4SO . It is not clear if these species were in the ice as such or if they originate from the fragmentation of larger species. But certainly, the signal recorded at $m/z = 50$ (H_2SO^+) or 49 (HSO $^+$) can be associated with the electron impact ionization of HSOH, while the signal attributed to species with gross formula CH_4SO (already identified also in the quiet coma) can be associated with mercaptomethanol, methyl thioperoxide, and methyl sulfenic acid formed in cometary ice. Finally, the record of SO with the same abundance as SO $_2$ (alleged to be its parent molecule) clearly indicates that there must be additional sources of SO. Except for OCS, CHOS, CH_4OS , and CH_3O_2S , no other molecules holding O, C, and S atoms were observed by the same instrument in the coma before the dust emission event.

6. Conclusions

This work indicates that the collisions between S(1D) and H_2O can be reactive since there is an open channel whose pathway evolves via intermediates and transition states below the reactants energy asymptote. To date, it has been included in the models of cometary comae only as a process inducing physical quenching. This is similar to the case of other collisions with water molecules, such as those of N(2D) that still in recent works are considered to be non-reactive while they easily lead to $HNO + H$ and $OH + NH$. The S(1D) + H_2O reaction can be a prompt source of SO under the denser conditions of the coma, close to the nucleus. The reaction with methanol does not seem to increase the degree of complexity of S-bearing molecules when it occurs in the gas phase.

To simulate the two reactions occurring in ice or liquid water, we have also considered them in the presence of four additional water molecules. The conclusion is that the initial

intermediates formed by the insertion or addition mechanism – namely HOSH (hydrogen thioperoxide) and H₂OS for S(¹D) + H₂O and CH₂OHSH (mercaptomethanol), CH₄OS and CH₃OSH (methyl thioperoxide) for S(¹D) + CH₃OH, as well as CH₃SOH (methyl sulfenic acid) for O(¹D) + CH₃SH – will probably be stabilized by the interaction with surrounding water molecules. Since this is an oversimplified model of ice, we are now pursuing a more realistic characterization of the S(¹D) + H₂O reaction in ice by using the methodology implemented by Rimola and coworkers (see, for instance,^{113,114}).

Our results can help in understanding the sulfur chemistry in space, especially in the case of comets. On one side, the gas-phase reaction S(¹D) + H₂O could account for the additional SO source necessary to explain its distribution in the Hale Bopp comet as resulting from an interferometric investigation. On the other side, some of the S/O-containing molecules identified by ROSINA during the enhanced dust emission events of the 67/P comet (e.g. species with gross formula HSO, H₂SO, and CH₄OS) could be the results of the chemistry occurring on ice that we have exposed in this work.

We urge modelers dealing with cometary chemistry to consider the reactive nature of S(¹D) + H₂O (as well as that of N(²D) + H₂O) in their models and to update the photodissociation schemes of S(¹D) mother molecules (especially H₂S and SO₂) as recently established by Cook et al.⁴⁰ and Chang et al.⁴²

Acknowledgement

The authors thank the Italian MUR PRIN2020 (2020AFB3FX-Astrochemistry beyond the second period elements) and the European Union's Horizon 2020 research and innovation program from the European Research Council (ERC) (project 'The Dawn of Organic Chemistry' DOC, grant agreement No 741002) for support. Support from the Italian Space Agency (Bando ASI Prot. n. DC-DSR-UVS-2022-231, Grant no. 2023-10-U.0 MIGLIORA) is also acknowledged.

AG and MR acknowledge financial support under the National Recovery and Resilience Plan (NRRP), Mission 4, Component 2, Investment 1.1, Call for tender No. 104 published on 2.2.2022 by the Italian Ministry of University and Research (MUR), funded by the European Union – NextGenerationEU– Project Title 2022JC2Y93 ChemicalOrigins: linking the fossil composition of the Solar System with the chemistry of protoplanetary disks – CUP J53D23001600006 - Grant Assignment Decree No. 962 adopted on 30.06.2023 by the Italian Ministry of Ministry of University and Research (MUR).

Supporting Information Available

- Tables S1-S5: electronic single-point energies for the systems: S(¹D) + H₂O (isolated), S(¹D) + CH₃OH (isolated), S(¹D) + H₂O in the presence of four additional water molecules, S(¹D) + CH₃OH in the presence of four additional water molecules.
- Cartesian and Internal coordinates of the structures of the identified intermediates, transition states and products.
- Figures S1-S2: optimized structures of the identified intermediates, transition states and products.

References

- (1) Fuente, A. et al. Gas phase Elemental abundances in Molecular cloudS (GEMS). VII. Sulfur elemental abundance. *Astronomy & Astrophysics* **2023**, 670, A114.
- (2) McGuire, B. A. 2021 Census of Interstellar, Circumstellar, Extragalactic, Protoplanetary Disk, and Exoplanetary Molecules. *The Astrophysical Journal Supplement Series* **2022**, 259, 30.

- (3) Jiménez-Escobar, A.; Muñoz Caro, G. M. Sulfur depletion in dense clouds and circumstellar regions. I. H₂S ice abundance and UV-photochemical reactions in the H₂O-matrix. *Astronomy & Astrophysics* **2011**, *536*, A91.
- (4) Jiménez-Escobar, A.; Muñoz Caro, G.; Chen, Y.-J. Sulphur depletion in dense clouds and circumstellar regions. Organic products made from UV photoprocessing of realistic ice analogs containing H₂S. *Monthly Notices of the Royal Astronomical Society* **2014**, *443*, 343–354.
- (5) Martín-Doménech, R.; Jiménez-Serra, I.; Muñoz Caro, G. M.; Müller, H. S. P.; Occhiogrosso, A.; Testi, L.; Woods, P. M.; Viti, S. The sulfur depletion problem: upper limits on the H₂S₂, HS₂, and S₂ gas-phase abundances toward the low-mass warm core IRAS 16293-2422. *Astronomy & Astrophysics* **2016**, *585*, A112.
- (6) Woods, P. M.; Occhiogrosso, A.; Viti, S.; Kaňuchová, Z.; Palumbo, M. E.; Price, S. D. A new study of an old sink of sulphur in hot molecular cores: the sulphur residue. *Monthly Notices of the Royal Astronomical Society* **2015**, *450*, 1256–1267.
- (7) Laas, J. C.; Caselli, P. Modeling sulfur depletion in interstellar clouds. *Astronomy & Astrophysics* **2019**, *624*, A108.
- (8) Navarro-Almaida, D.; Le Gal, R.; Fuente, A.; Rivière-Marichalar, P.; Wakelam, V.; Cazaux, S.; Caselli, P.; Laas, J. C.; Alonso-Albi, T.; Loison, J.; others Gas phase Elemental abundances in Molecular cloudS (GEMS)-II. On the quest for the sulphur reservoir in molecular clouds: the H₂S case. *Astronomy & Astrophysics* **2020**, *637*, A39.
- (9) Boogert, A. A.; Gerakines, P. A.; Whittet, D. C. Observations of the Icy Universe. *Annual Review of Astronomy and Astrophysics* **2015**, *53*, 541–581.
- (10) Boogert, A.; Brewer, K.; Brittain, A.; Emerson, K. Survey of ices toward massive

young stellar objects. I. OCS, CO, OCN⁻, and CH₃OH. *The Astrophysical Journal* **2022**, *941*, 32.

- (11) McClure, M. K.; Rocha, W.; Pontoppidan, K.; Crouzet, N.; Chu, L. E.; Dartois, E.; Lamberts, T.; Noble, J.; Pendleton, Y.; Perotti, G.; others An Ice Age JWST inventory of dense molecular cloud ices. *Nature astronomy* **2023**, *7*, 431–443.
- (12) Bariosco, V.; Pantaleone, S.; Ceccarelli, C.; Rimola, A.; Balucani, N.; Corno, M.; Ugliengo, P. The binding energy distribution of H₂S: why it is not the major sulphur reservoir of the interstellar ices. *Monthly Notices of the Royal Astronomical Society* **2024**, *531*, 1371–1384.
- (13) Smith, A. M.; Stecher, T. P.; Casswell, L. Production of carbon, sulfur, and CS in Comet West. *Astrophysical Journal* **1980**, *242*, 402–410.
- (14) Bockelée-Morvan, D.; Colom, P.; Crovisier, J.; Despois, D.; Paubert, G. Microwave detection of hydrogen sulphide and methanol in comet Austin (1989c1). *Nature* **1991**, *350*, 318–320.
- (15) Woodney, L.; A'hearn, M.; McMullin, J.; Samarasinha, N. Sulfur chemistry at millimeter wavelengths in C/Hale-Bopp. *Earth, Moon, and Planets* **1997**, *78*, 69.
- (16) Woodney, L.; McMullin, J.; A'Hearn, M. Detection of OCS in comet Hyakutake (C/1996 B2). *Planetary and space science* **1997**, *45*, 717–719.
- (17) A'Hearn, M. F.; Schleicher, D. G.; Feldman, P. D. The discovery of S₂ in comet IRAS-Araki-Alcock 1983d. *Astrophysical Journal, Letters* **1983**, *274*, L99–L103.
- (18) Bockelée-Morvan, D. et al. New molecules found in comet C/1995 O1 (Hale-Bopp). Investigating the link between cometary and interstellar material. *Astronomy & Astrophysics* **2000**, *353*, 1101–1114.

- (19) Jackson, W. M.; Scodinu, A.; Xu, D.; Cochran, A. L. Using the Ultraviolet and Visible spectrum of Comet 122P/de Vico to Identify the Parent Molecule CS₂. *Astrophysical Journal, Letters* **2004**, *607*, L139–L141.
- (20) Irvine, W. M.; Senay, M.; Lovell, A. J.; Matthews, H. E.; McGonagle, D.; Meier, R. NOTE: Detection of Nitrogen Sulfide in Comet Hale-Bopp. *Icarus* **2000**, *143*, 412–414.
- (21) Mumma, M. J.; Charnley, S. B. The Chemical Composition of Comets—Emerging Taxonomies and Natal Heritage. *Annual Review of Astronomy and Astrophysics* **2011**, *49*, 471–524.
- (22) Crovisier, J.; Bockelée-Morvan, D. Remote Observations of the Composition of Cometary Volatiles. *Space Science Reviews* **1999**, *90*, 19–32.
- (23) Crovisier, J.; Bockelée-Morvan, D.; Colom, P.; Biver, N.; Despois, D.; Lis, D. C.; Target-of-opportunity Radio Observations of Comets Team The composition of ices in comet C/1995 O1 (Hale-Bopp) from radio spectroscopy. Further results and upper limits on undetected species. *Astronomy & Astrophysics* **2004**, *418*, 1141–1157.
- (24) Le Roy, L.; Altwegg, K.; Balsiger, H.; Berthelier, J.-J.; Bieler, A.; Briois, C.; Calmonte, U.; Combi, M. R.; De Keyser, J.; Dhooghe, F.; others Inventory of the volatiles on comet 67P/Churyumov-Gerasimenko from Rosetta/ROSINA. *Astronomy & Astrophysics* **2015**, *583*, A1.
- (25) Calmonte, U.; Altwegg, K.; Balsiger, H.; Berthelier, J.-J.; Bieler, A.; Cessateur, G.; Dhooghe, F.; Van Dishoeck, E.; Fiethe, B.; Fuselier, S.; others Sulphur-bearing species in the coma of comet 67P/Churyumov–Gerasimenko. *Monthly Notices of the Royal Astronomical Society* **2016**, *462*, S253–S273.
- (26) Altwegg, K.; Balsiger, H.; Fuselier, S. A. Cometary chemistry and the origin of icy solar system bodies: the view after Rosetta. *Annual Review of Astronomy and Astrophysics* **2019**, *57*, 113–155.

- (27) Hänni, N.; Altwegg, K.; Combi, M.; Fuselier, S.; De Keyser, J.; Rubin, M.; Wampfler, S. Identification and characterization of a new ensemble of cometary organic molecules. *Nature Communications* **2022**, *13*, 3639.
- (28) Mahjoub, A.; Altwegg, K.; Poston, M. J.; Rubin, M.; Hodyss, R.; Choukroun, M.; Ehlmann, B. L.; Hänni, N.; Brown, M. E.; Blacksberg, J.; Eiler, J. M.; Hand, K. P. Complex organosulfur molecules on comet 67P: Evidence from the ROSINA measurements and insights from laboratory simulations. *Science Advances* **2023**, *9*, eadh0394.
- (29) Altwegg, K.; Combi, M.; Fuselier, S.; Hänni, N.; De Keyser, J.; Mahjoub, A.; Müller, D. R.; Pestoni, B.; Rubin, M.; Wampfler, S. Abundant ammonium hydrosulfide embedded in cometary dust grains. *Monthly Notices of the Royal Astronomical Society* **2022**, *516*, 3900–3910.
- (30) Schmitt-Kopplin, P.; Hertkorn, N.; Harir, M.; Moritz, F.; Lucio, M.; Bonal, L.; Quirico, E.; Takano, Y.; Dworkin, J. P.; Naraoka, H.; others Soluble organic matter Molecular atlas of Ryugu reveals cold hydrothermalism on C-type asteroid parent body. *Nature communications* **2023**, *14*, 6525.
- (31) Naraoka, H. et al. Soluble organic molecules in samples of the carbonaceous asteroid (162173) Ryugu. *Science* **2023**, *379*, eabn9033.
- (32) Yoshimura, T. et al. Chemical evolution of primordial salts and organic sulfur molecules in the asteroid 162173 Ryugu. *Nature Communications* **2023**, *14*.
- (33) Zhrebker, A.; Kostyukevich, Y.; Volkov, D. S.; Chumakov, R. G.; Friederici, L.; Rüger, C. P.; Kononikhin, A.; Kharybin, O.; Korochantsev, A.; Zimmermann, R.; Perminova, I. V.; Nikolaev, E. Speciation of organosulfur compounds in carbonaceous chondrites. *Scientific Reports* **2021**, *11*, 7410.
- (34) Chyba, C.; Sagan, C. Endogenous production, exogenous delivery and impact-shock

- synthesis of organic molecules: an inventory for the origins of life. *Nature* **1992**, *355*, 125–132.
- (35) Schofield, K. Critically evaluated rate constants for gaseous reactions of several electronically excited species. *Journal of Physical and Chemical Reference Data* **1979**, *8*, 723–798.
- (36) Nan, G.; Burak, I.; Houston, P. Photodissociation of OCS at 222 nm. The triplet channel. *Chemical Physics Letters* **1993**, *209*, 383–389.
- (37) Kitsopoulos, T. N.; Gebhardt, C. R.; Rakitzis, T. P. Photodissociation study of CS₂ at 193 nm using slice imaging. *The Journal of Chemical Physics* **2001**, *115*, 9727–9732.
- (38) McGivern, W. S.; Sorkhabi, O.; Rizvi, A. H.; Suits, A. G.; North, S. W. Photofragment translational spectroscopy with state-selective universal detection: The ultraviolet photodissociation of CS₂. *The Journal of Chemical Physics* **2000**, *112*, 5301–5307.
- (39) Sun, Z.; Farooq, Z.; Parker, D.; Martin, P.; Western, C. Photodissociation of S₂ ($X_3\Sigma_g^-$, $a_1\Delta_g$, and $b_1\Sigma_g^+$) in the 320–205 nm Region. *The Journal of Physical Chemistry A* **2019**, *123*, 6886–6896.
- (40) Cook, P. A.; Langford, S. R.; Dixon, R. N.; Ashfold, M. N. An experimental and ab initio reinvestigation of the Lyman- α photodissociation of H₂S and D₂S. *The Journal of Chemical Physics* **2001**, *114*, 1672–1684.
- (41) Zhao, Y.; Luo, Z.; Chang, Y.; Wu, Y.; Zhang, S.-e.; Li, Z.; Ding, H.; Wu, G.; Campbell, J. S.; Hansen, C. S.; others Rotational and nuclear-spin level dependent photodissociation dynamics of H₂S. *Nature Communications* **2021**, *12*, 4459.
- (42) Chang, Y.; Fu, Y.; Chen, Z.; Luo, Z.; Zhao, Y.; Li, Z.; Zhang, W.; Wu, G.; Fu, B.; Zhang, D. H.; Ashfold, M. N. R.; Yang, X.; Yuan, K. Vacuum ultraviolet photodissoci-

ation of sulfur dioxide and its implications for oxygen production in the early Earth's atmosphere. *Chemical Science* **2023**, *14*, 8255–8261.

- (43) Carder, J. T.; Ochs, W.; Herbst, E. Modelling the insertion of O(¹D) into methane on the surface of interstellar ice mantles. *Monthly Notices of the Royal Astronomical Society* **2021**, *508*, 1526–1532.
- (44) Bergner, J. B.; Öberg, K. I.; Rajappan, M. Methanol formation via oxygen insertion chemistry in ices. *The Astrophysical Journal* **2017**, *845*, 29.
- (45) Bergner, J. B.; Öberg, K. I.; Rajappan, M. Oxygen atom reactions with C₂H₆, C₂H₄, and C₂H₂ in ices. *The Astrophysical Journal* **2019**, *874*, 115.
- (46) Daniely, A.; Zamir, A.; Eisenberg, H. R.; Livshits, E.; Piacentino, E.; Bergner, J. B.; Oberg, K.; Stein, T. Singlet Oxygen Insertion into Hydrocarbons: The Role of First- and Second-Generation Pathways in Astronomically Relevant Ices. *Theoretical and Computational Chemistry*, doi: 10.26434/chemrxiv-2024-pddc0 **2024**,
- (47) Kjellström, E. A three-dimensional global model study of carbonyl sulfide in the troposphere and the lower stratosphere. *Journal of Atmospheric Chemistry* **1998**, *29*, 151–177.
- (48) Karu, E.; Li, M.; Ernle, L.; Brenninkmeijer, C. A. M.; Lelieveld, J.; Williams, J. Carbonyl Sulfide (OCS) in the Upper Troposphere/Lowermost Stratosphere (UT/LMS) Region: Estimates of Lifetimes and Fluxes. *Geophysical Research Letters* **2023**, *50*, e2023GL105826, e2023GL105826 2023GL105826.
- (49) Kim, M. H.; Li, W.; Lee, S. K.; Suits, A. G. Probing of the hot-band excitations in the photodissociation of OCS at 288 nm by DC slice imaging. *Canadian Journal of Chemistry* **2004**, *82*, 880–884.

- (50) Katayanagi, H.; Mo, Y.; Suzuki, T. 223 nm photodissociation of OCS. Two components in S(¹D₂) and S(³P₂) channels. *Chemical Physics Letters* **1995**, *247*, 571–576.
- (51) Leonori, F.; Petrucci, R.; Balucani, N.; Casavecchia, P.; Rosi, M.; Skouteris, D.; Berteloite, C.; Le Picard, S. D.; Canosa, A.; Sims, I. R. Crossed-beam dynamics, low-temperature kinetics, and theoretical studies of the reaction S(¹D) + C₂H₄. *The Journal of Physical Chemistry A* **2009**, *113*, 15328–15345.
- (52) Leonori, F.; Petrucci, R.; Balucani, N.; Casavecchia, P.; Rosi, M.; Berteloite, C.; Le Picard, S. D.; Canosa, A.; Sims, I. R. Observation of organosulfur products (thiovinoxy, thioketene and thioformyl) in crossed-beam experiments and low temperature rate coefficients for the reaction S(¹D) + C₂H₄. *Physical Chemistry Chemical Physics* **2009**, *11*, 4701–4706.
- (53) Leonori, F.; Petrucci, R.; Balucani, N.; Hickson, K. M.; Hamberg, M.; Geppert, W. D.; Casavecchia, P.; Rosi, M. Crossed-beam and theoretical studies of the S(¹D) + C₂H₂ reaction. *The Journal of Physical Chemistry A* **2009**, *113*, 4330–4339.
- (54) Berteloite, C.; Le Picard, S. D.; Sims, I. R.; Rosi, M.; Leonori, F.; Petrucci, R.; Balucani, N.; Wang, X.; Casavecchia, P. Low temperature kinetics, crossed beam dynamics and theoretical studies of the reaction S(¹D) + CH₄ and low temperature kinetics of S(¹D) + C₂H₂. *Physical Chemistry Chemical Physics* **2011**, *13*, 8485–8501.
- (55) Balucani, N.; Leonori, F.; Petrucci, R.; Casavecchia, P.; Skouteris, D.; Rosi, M. Experimental and theoretical studies on possible formation routes of organosulfur compounds in extraterrestrial environments. *Memorie della Societa Astronomica Italiana Supplement* **2011**, *16*, 91.
- (56) Leonori, F.; Skouteris, D.; Petrucci, R.; Casavecchia, P.; Rosi, M.; Balucani, N. Combined crossed beam and theoretical studies of the C(¹D)+ CH₄ reaction. *The Journal of Chemical Physics* **2013**, *138*.

- (57) Kaiser, R. I.; Nguyen, T. L.; Mebel, A. M.; Lee, Y. T. Stripping dynamics in the reactions of electronically excited carbon atoms, C(¹D), with ethylene and propylene—production of propargyl and methylpropargyl radicals. *The Journal of Chemical Physics* **2002**, *116*, 1318–1324.
- (58) Balucani, N.; Bergeat, A.; Cartechini, L.; Volpi, G. G.; Casavecchia, P.; Skouteris, D.; Rosi, M. Combined crossed molecular beam and theoretical studies of the N(²D)+ CH₄ reaction and implications for atmospheric models of Titan. *The Journal of Physical Chemistry A* **2009**, *113*, 11138–11152.
- (59) Homayoon, Z.; Bowman, J. M.; Balucani, N.; Casavecchia, P. Quasiclassical trajectory calculations of the N(²D)+ H₂O reaction elucidating the formation mechanism of HNO and HON seen in molecular beam experiments. *The Journal of Physical Chemistry Letters* **2014**, *5*, 3508–3513.
- (60) Balucani, N.; Caracciolo, A.; Vanuzzo, G.; Skouteris, D.; Rosi, M.; Pacifici, L.; Casavecchia, P.; Hickson, K. M.; Loison, J.-C.; Dobrijevic, M. An experimental and theoretical investigation of the N(²D)+ C₆H₆ (benzene) reaction with implications for the photochemical models of Titan. *Faraday Discussions* **2023**, *245*, 327–351.
- (61) Balucani, N.; Skouteris, D.; Leonori, F.; Petrucci, R.; Hamberg, M.; Geppert, W. D.; Casavecchia, P.; Rosi, M. Combined crossed beam and theoretical studies of the N(²D)+ C₂H₄ reaction and implications for atmospheric models of Titan. *The Journal of Physical Chemistry A* **2012**, *116*, 10467–10479.
- (62) Biver, N. et al. Molecular composition of short-period comets from millimetre-wave spectroscopy: 21P/Giacobini-Zinner, 38P/Stephan-Oterma, 41P/Tuttle-Giacobini-Kresák, and 64P/Swift-Gehrels. *Astronomy and Astrophysics* **2021**, *651*, A25.
- (63) Cordiner, M. A.; Roth, N. X.; Milam, S. N.; Villanueva, G. L.; Bockelée-Morvan, D.; Remijan, A. J.; Charnley, S. B.; Biver, N.; Lis, D. C.; Qi, C.; Bonev, B. P.; Crovisier, J.;

Boissier, J. Gas Sources from the Coma and Nucleus of Comet 46P/Wirtanen Observed Using ALMA. *The Astrophysical Journal* **2023**, *953*, 59.

- (64) Lippi, M.; Podio, L.; Codella, C.; Faggi, S.; Simone, M. D.; Villanueva, G. L.; Mumma, M. J.; Ceccarelli, C. The Ice Chemistry in Comets and Planet-forming Disks: Statistical Comparison of CH₃OH, H₂CO, and NH₃ Abundance Ratios. *The Astrophysical Journal Letters* **2024**, *970*, L5.
- (65) Opitom, C.; Hutsemékers, D.; Jehin, E.; Rousselot, P.; Pozuelos, F. J.; Manfroid, J.; Moulane, Y.; Gillon, M.; Benkhaldoun, Z. High resolution optical spectroscopy of the N₂-rich comet C/2016 R2 (PanSTARRS). *Astronomy and Astrophysics* **2019**, *624*, A64.
- (66) Raghuram, S.; Hutsemékers, D.; Opitom, C.; Jehin, E.; Bhardwaj, A.; Manfroid, J. Forbidden atomic carbon, nitrogen, and oxygen emission lines in the water-poor comet C/2016 R2 (Pan-STARRS). *Astronomy and Astrophysics* **2020**, *635*, A108.
- (67) Lupu, R. E.; Feldman, P. D.; Weaver, H. A.; Tozzi, G.-P. The Fourth Positive System of Carbon Monoxide in the Hubble Space Telescope Spectra of Comets. *The Astrophysical Journal* **2007**, *670*, 1473.
- (68) A'Hearn, M. F.; Arpigny, C.; Feldman, P. D.; Jackson, W. M.; Meier, R.; Weaver, H. A.; Wellnitz, D. D.; Woodney, L. M. Formation of S₂ in Comets. AAS/Division for Planetary Sciences Meeting Abstracts #32. 2000; p 44.01.
- (69) Rodgers, S.; Charnley, S. Sulfur chemistry in cometary comae. *Advances in Space Research* **2006**, *38*, 1928–1931.
- (70) Schmidt, H. U.; Wegmann, R.; Huebner, W. F.; Boice, D. C. Cometary gas and plasma flow with detailed chemistry. *Computer Physics Communications* **1988**, *49*, 17–59.

- (71) Atkinson, R.; Baulch, D. L.; Cox, R. A.; Crowley, J. N.; Hampson, R. F.; Hynes, R. G.; Jenkin, M. E.; Rossi, M. J.; Troe, J. Evaluated kinetic and photochemical data for atmospheric chemistry: Volume I - gas phase reactions of O_x, HO_x, NO_x and SO_x species. *Atmospheric Chemistry and Physics* **2004**, *4*, 1461–1738.
- (72) Chai, J.-D.; Head-Gordon, M. Long-range corrected hybrid density functionals with damped atom–atom dispersion corrections. *Physical Chemistry Chemical Physics* **2008**, *10*, 6615.
- (73) Dunning Jr, T. H. Gaussian basis sets for use in correlated molecular calculations. I. The atoms boron through neon and hydrogen. *The Journal of chemical physics* **1989**, *90*, 1007–1023.
- (74) Dunning Jr, T. H.; Peterson, K. A.; Wilson, A. K. Gaussian basis sets for use in correlated molecular calculations. X. The atoms aluminum through argon revisited. *The Journal of Chemical Physics* **2001**, *114*, 9244–9253.
- (75) Raghavachari, K.; Trucks, G. W.; Pople, J. A.; Head-Gordon, M. A fifth-order perturbation comparison of electron correlation theories. *Chemical Physics Letters* **1989**, *157*, 479–483.
- (76) Bartlett, R. J. Many-Body Perturbation Theory and Coupled Cluster Theory for Electron Correlation in Molecules. *Annual Review of Physical Chemistry* **1981**, *32*, 359–401.
- (77) Frisch, M. et al. Gaussian 09, Revision A. 02, 2009, Gaussian. Inc., Wallingford CT **2009**,
- (78) Fukui, K. The path of chemical reactions—the IRC approach. *Accounts of chemical research* **1981**, *14*, 363–368.

- (79) Werner, H.-J.; Knowles, P. J.; Manby, F. R.; Black, J. A.; Doll, K.; Heßelmann, A.; Kats, D.; Köhn, A.; Korona, T.; Kreplin, D. A.; others The Molpro quantum chemistry package. *The Journal of chemical physics* **2020**, *152*, 144107.
- (80) Wilson, A. K.; Dunning, T. H. The HSO-SOH Isomers Revisited: The Effect of Tight d Functions. *The Journal of Physical Chemistry A* **2004**, *108*, 3129–3133.
- (81) Martin, J. M. Ab initio total atomization energies of small molecules — towards the basis set limit. *Chemical Physics Letters* **1996**, *259*, 669–678.
- (82) Moore, C. *Atomic Energy Levels, Vol. 1*; Circular of the National Bureau of Standards 467; U.S. Government Printing Office, 1949.
- (83) Becke, A. D. Density-functional thermochemistry. I. The effect of the exchange-only gradient correction. *The Journal of chemical physics* **1992**, *96*, 2155–2160.
- (84) Becke, A. D. Density-functional thermochemistry. III. The role of exact exchange. *The Journal of Chemical Physics* **1993**, *98*, 5648–5652.
- (85) Vanuzzo, G.; Mancini, L.; Pannacci, G.; Liang, P.; Marchione, D.; Recio, P.; Tan, Y.; Rosi, M.; Skouteris, D.; Casavecchia, P.; Balucani, N.; Hickson, K. M.; Loison, J.-C.; Dobrijevic, M. Reaction N(2D) + CH₂CCH₂ (Allene): An Experimental and Theoretical Investigation and Implications for the Photochemical Models of Titan. *ACS Earth and Space Chemistry* **2022**, *6*, 2305–2321.
- (86) Goumri, A.; Rocha, J. R.; Laakso, D.; Smith, C. E.; Marshall, P. Computational studies of the potential energy surface for O(¹D) + H₂S: Characterization of pathways involving H₂SO, HOSH, and H₂OS. *The Journal of Chemical Physics* **1994**, *101*, 9405–9411.
- (87) Borin, A. C.; Ornellas, F. R. The lowest triplet and singlet electronic states of the molecule SO. *Chemical physics* **1999**, *247*, 351–364.

- (88) Ruscic, B.; Pinzon, R. E.; Morton, M. L.; von Laszewski, G.; Bittner, S. J.; Nijssure, S. G.; Amin, K. A.; Minkoff, M.; Wagner, A. F. Introduction to Active Thermochemical Tables: Several “Key” Enthalpies of Formation Revisited. *The Journal of Physical Chemistry A* **2004**, *108*, 9979–9997.
- (89) Nagy, B.; Szakács, P.; Csontos, J.; Rolik, Z.; Tasi, G.; Kállay, M. High-Accuracy Theoretical Thermochemistry of Atmospherically Important Sulfur-Containing Molecules. *The Journal of Physical Chemistry A* **2011**, *115*, 7823–7833.
- (90) Resende, S. M.; Ornellas, F. R. Thermochemistry of atmospheric sulfur compounds. *Chemical Physics Letters* **2003**, *367*, 489–494.
- (91) Giustini, A.; Di Genova, G.; Balucani, N.; Ceccarelli, C.; Rosi, M.; Lombardi, A. Theoretical Insights on the S(¹D) + H₂O Reaction and Implications on the Chemistry at the Surface of Ice in Extraterrestrial Environments. Computational Science and Its Applications – ICCSA 2024 Workshops. Cham, 2024; pp 274–282.
- (92) Rosi, M.; Balucani, N.; Casavecchia, P.; Mancini, L.; Pannacci, G.; Vanuzzo, G. A Computational Strategy for the Theoretical Investigation of the Reactions Between Atomic Oxygen and Aromatic Compounds. Computational Science and Its Applications – ICCSA 2024 Workshops. Cham, 2024; pp 1–13.
- (93) Enrique-Romero, J.; Rimola, A.; Ceccarelli, C.; Ugliengo, P.; Balucani, N.; Skouteris, D. Quantum mechanical simulations of the radical–radical chemistry on icy surfaces. *The Astrophysical Journal Supplement Series* **2022**, *259*, 39.
- (94) Pantaleone, S.; Enrique-Romero, J.; Ceccarelli, C.; Ferrero, S.; Balucani, N.; Rimola, A.; Ugliengo, P. H₂ formation on interstellar grains and the fate of reaction energy. *The Astrophysical Journal* **2021**, *917*, 49.
- (95) Pantaleone, S.; Enrique-Romero, J.; Ceccarelli, C.; Ugliengo, P.; Balucani, N.; Rimola, A.; Ugliengo, P. H₂ formation on interstellar grains and the fate of reaction energy. *The Astrophysical Journal* **2021**, *917*, 49.

- mola, A. Chemical desorption versus energy dissipation: Insights from ab initio molecular dynamics of HCO⁺-formation. *The Astrophysical Journal* **2020**, *897*, 56.
- (96) Balucani, N.; Cartechini, L.; Casavecchia, P.; Homayoon, Z.; Bowman, J. M. A combined crossed molecular beam and quasiclassical trajectory study of the Titan-relevant N(²D)+ D₂O reaction. *Molecular Physics* **2015**, *113*, 2296–2301.
- (97) Umemoto, H.; Kongo, K.; Inaba, S.; Sonoda, Y.; Takayanagi, T.; Kurosaki, Y. Reactions of N(²D) with CH₃OH and Its Isotopomers. *The Journal of Physical Chemistry A* **1999**, *103*, 7026–7031.
- (98) Black, G. Branching ratios for quenching and reaction in the interaction of S (¹D₂) with various gases. *The Journal of chemical physics* **1986**, *84*, 1345–1348.
- (99) Fowles, P.; deSorgo, M.; Yarwood, A. J.; Strausz, O. P.; Gunning, H. E. The Reactions of sulfur Atoms. IX. The Flash Photolysis of Carbonyl Sulfide and the Reactions of S(¹D) Atoms with Hydrogen and Methane. *Journal of the American Chemical Society* **1967**, *89*, 1352–1362.
- (100) Lang, J.; Foley, C. D.; Thawoos, S.; Behzadfar, A.; Liu, Y.; Zádor, J.; Suits, A. G. Reaction dynamics of S (3 P) with 1, 3-butadiene and isoprene: crossed-beam scattering, low-temperature flow experiments, and high-level electronic structure calculations. *Faraday Discussions* **2024**,
- (101) Li, H.; Lang, J.; Foley, C. D.; Zádor, J.; Suits, A. G. Sulfur (3P) Reaction with Conjugated Dienes Gives Cyclization to Thiophenes under Single Collision Conditions. *The Journal of Physical Chemistry Letters* **2023**, *14*, 7611–7617.
- (102) Doddipatla, S.; He, C.; Goettl, S. J.; Kaiser, R. I.; Galvão, B. R.; Millar, T. J. Nonadiabatic reaction dynamics to silicon monosulfide (SiS): A key molecular building block to sulfur-rich interstellar grains. *Science Advances* **2021**, *7*, eabg7003.

- (103) Balucani, N.; Beneventi, L.; Casavecchia, P.; Stranges, D.; Volpi, G. The effect of reagent electronic energy on the dynamics of chemical reactions: A high-resolution crossed beam study of O (3P , 1D) + H₂S. *The Journal of Chemical Physics* **1991**, *94*, 8611–8614.
- (104) Balucani, N.; Stranges, D.; Casavecchia, P.; Volpi, G. G. Crossed beam studies of the reactions of atomic oxygen in the ground 3P and first electronically excited 1D states with hydrogen sulfide. *The Journal of Chemical Physics* **2004**, *120*, 9571–9582.
- (105) Cavallotti, C.; De Falco, C.; Pratali Maffei, L.; Caracciolo, A.; Vanuzzo, G.; Balucani, N.; Casavecchia, P. Theoretical study of the extent of intersystem crossing in the O(3P) + C₆H₆ reaction with experimental validation. *The Journal of Physical Chemistry Letters* **2020**, *11*, 9621–9628.
- (106) Recio, P.; Alessandrini, S.; Vanuzzo, G.; Pannacci, G.; Baggio, A.; Marchione, D.; Caracciolo, A.; Murray, V. J.; Casavecchia, P.; Balucani, N.; others Intersystem crossing in the entrance channel of the reaction of O(3P) with pyridine. *Nature Chemistry* **2022**, *14*, 1405–1412.
- (107) Balucani, N.; Vanuzzo, G.; Recio, P.; Caracciolo, A.; Rosi, M.; Cavallotti, C.; Baggio, A.; Della Libera, A.; Casavecchia, P. Crossed molecular beam experiments and theoretical simulations on the multichannel reaction of toluene with atomic oxygen. *Faraday Discuss.* **2024**, doi:10.1039/D3FD00181D.
- (108) Lara, M.; Berteloite, C.; Paniagua, M.; Dayou, F.; Launay, J.-M. Experimental and theoretical study of the collisional quenching of S (1D) by Ar. *Physical Chemistry Chemical Physics* **2017**, *19*, 28555–28571.
- (109) Herbst, E. An approach to the estimation of polyatomic vibrational radiative relaxation rates. *Chemical Physics* **1982**, *65*, 185–195.

- (110) Herbst, E. Unusual Chemical Processes in Interstellar Chemistry: Past and Present. *Frontiers in Astronomy and Space Sciences* **2021**, *8*.
- (111) Boissier, J.; Bockelée-Morvan, D.; Biver, N.; Crovisier, J.; Despois, D.; Marsden, B.; Moreno, R. Interferometric imaging of the sulfur-bearing molecules HS, SO, and CS in comet C/1995 O1 (Hale-Bopp). *Astronomy & Astrophysics* **2007**, *475*, 1131–1144.
- (112) Góbi, S.; Csonka, I. P.; Bazsó, G.; Tarczay, G. Successive Hydrogenation of SO and SO₂ in Solid para-H₂: Formation of Elusive Small Oxoacids of Sulfur. *ACS Earth and Space Chemistry* **2021**, *5*, 1180–1195.
- (113) Perrero, J.; Enrique-Romero, J.; Martínez-Bachs, B.; Ceccarelli, C.; Balucani, N.; Ugliengo, P.; Rimola, A. Non-energetic formation of ethanol via CCH reaction with interstellar H₂O ices. A computational chemistry study. *ACS Earth and Space Chemistry* **2022**, *6*, 496–511.
- (114) Rimola, A.; Skouteris, D.; Balucani, N.; Ceccarelli, C.; Enrique-Romero, J.; Taquet, V.; Ugliengo, P. Can formamide be formed on interstellar ice? An atomistic perspective. *ACS Earth and Space Chemistry* **2018**, *2*, 720–734.

TOC Graphic

